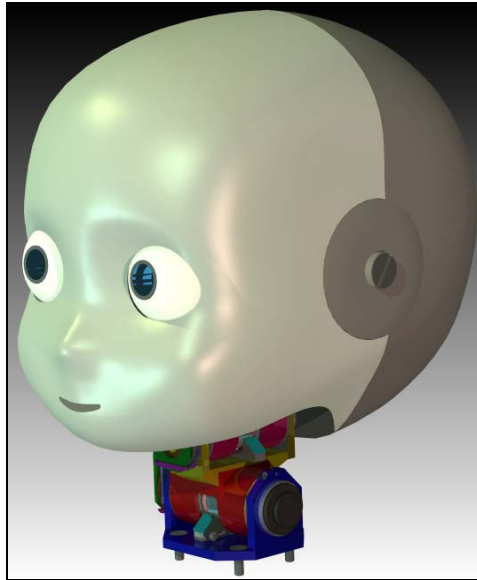




INSTITUTO
SUPERIOR
TÉCNICO

UNIVERSIDADE TÉCNICA DE LISBOA INSTITUTO SUPERIOR TÉCNICO



Mechanical Design of an Anthropomorphic Robot Head

Ricardo Beira

(Licenciado)

**Dissertação para obtenção do Grau de Mestre
em Engenharia de Conceção**

Orientador: Doutor José Alberto Rosado dos Santos Victor

Júri

Presidente: Doutor José Alberto Rosado dos Santos Victor

Vogais: Doutor Hélder de Jesus Araújo

Doutor Alexandre José Malheiro Bernardino

Doutor Arlindo José de Pinho Figueiredo e Silva

Janeiro 2008

Título: Projecto Mecânico de uma Cabeça Antropomórfica Robótica

Nome: Ricardo Daniel Rita Beira

Curso de Mestrado em: Engenharia de Concepção

Orientador: Professor José Santos Victor

Resumo

Esta tese tem como principal objectivo o uso de ferramentas computacionais e de cálculo para o projecto mecânico de um sistema robótico, composto por um pescoço e uma cabeça antropomórfica de um robot humanóide.

O trabalho foi desenvolvido no âmbito do Projecto Europeu RobotCub, que consiste num dos maiores esforços no sentido de desenvolver as capacidades de percepção e raciocínio dos robots, integrando equipas de engenharia bem como equipas de psicologia, medicina e neurociência, visando criar robots que desenvolvam as suas capacidades perceptuais, motoras e cognitivas ao longo do tempo, de forma semelhante ao desenvolvimento de crianças ou recém-nascidos, permitindo assim, testar os princípios subjacentes a esses mecanismos biológicos. A plataforma final, o iCub, terá aproximadamente 90 cm de altura, 23 kg de peso e um total de 53 graus de liberdade.

Para que esta cabeça robótica seja dotada de propriedades similares à de uma criança de dois anos, foi feito um levantamento, não só das várias especificações que o sistema biológico possui, do ponto de vista anatómico e comportamental, mas também das soluções utilizadas noutros robots já existentes.

No final, foi produzido um modelo funcional da plataforma, sendo testadas e optimizadas as suas performances mecânicas.

Palavras-chave: Robots Humanóides; Projecto Mecânico; Análises Dinâmicas; Selecção de Actuadores; Mecanismos Robóticos; Coordenação Visuomotora

Abstract

This Thesis's main objective was to develop an anthropomorphic robot head, composed by a neck and a vision system, using computational and analytical tools for its mechanical design.

The work was developed in the framework of the European Project RobotCub which is one of the biggest efforts to develop the capacities of perception and reasoning of robots. It integrates research groups of engineers as well as teams of psychology, medicine and neuroscience aiming to create robots can be able to develop their own perceptual, motor and cognitive capacities along the time, similar to the development of children or rear-born, thus allowing to test the underlying principles of these biological mechanisms. The final platform, the iCUB, is approximately 90 cm tall, with 23 kg and with a total number of 53 degrees of freedom.

So, as this robot head was designed to have similar properties of a two-year-old child's head, some specifications were based, not only on the other different solutions, used in several humanoid robots, but also on the biological system anatomical and behavioral data.

In the end, a platform prototype was produced, tested and optimized, in order to increase its mechanical performances.

Keywords: Humanoid Robots; Biologically Inspired Robots; Mechanical Design; Dynamic Analysis; Actuators Selection; Robotic Mechanisms; Visual-motor coordination

Acknowledgements

I would like to express my great admiration for Professor José Santos-Victor and appreciation for all the help he patiently gave, not only during the thesis project but through out all the MSc. period.

His general knowledge, expertise, methodology and humour greatly surpass the context of this thesis and it will certainly be invaluable to me through out my career.

Very special thanks to Miguel Praça, for the endless efforts in providing me with all the technical support to come through with this project. His initiative and work methodology has served me has an important source of inspiration.

I would like to thank also to my colleagues Manel, Vargas, Alex, Rui Santos, Rodrigo and Ricardo Nunes, for their dedication and friendship during this period.

Index

Resumo	I
Abstract.....	II
Acknowledgements	III
Index.....	1
1. Introduction	3
1.1. Research Context.....	3
1.2. Benchmarking	6
1.3. Our Approach	8
1.4. Thesis Organization	11
2. Head Specifications	13
2.1. Anatomical Data.....	13
2.2. Robot Head Specifications.....	18
3. Model Development	23
3.1. Neck Mechanism	24
3.1.1. Flexible Neck Solution	25
3.1.2. Parallel Mechanism Solution	27
3.1.3. Serial Mechanism Solution	34
3.2. Eyes Mechanism.....	38
3.3. Actuators Selection.....	40
3.4. Eyelid Mechanism	43
3.5. Material Selection	46
3.6. Assembly.....	47
3.7. Sensors and Electronics	49
3.6 External Cover.....	52
4. Performance	55
5. Conclusions/ Future Work	59
6. References.....	63

1. Introduction

This thesis describes the design of a robot head [Beira et al., 2005], developed in the framework of the RobotCub project [Sandini et al., 2004]. This project's goal consists on the design and construction of a humanoid robotic platform, the iCub, for the study of human cognition. The final platform will be approximately 90cm tall, with 23 kg and with a total number of 53 degrees of freedom.

For its size, the iCub is the most complete humanoid robot currently being designed, in terms of kinematic complexity. The eyes can also move, as opposed to similarly sized humanoid platforms.

Specifications were based on biological, anatomical and behavioural data, as well as tasks constraints. Different concepts for the neck design (flexible, parallel and serial solutions) were analyzed and compared with respect to the specifications. The eye and eyelids mechanical design is presented, as well as a description of the head external cover and electronics.

We also present the several tests made to evaluate the functional performances of the designed head.

1.1. Research Context

The first developments of humanoid mechanical platforms started in the mid-seventies in Japan, when the state of computing technology (but also sensors and vision, energy supply, etc.) was still far from what is needed even for a basic notion of "autonomy". Even though at that time we could not even dream of implementing higher-level cognitive abilities as integral functions of these bodies, there were impressive achievements of the emulation of human motor skills (walking, grasping, even piano-playing).

Throughout the 1980's engineering efforts went into human inspired limbs, particularly multi-fingered hands, but it faded away when it became clear that there are very few, if any, immediate industrial applications. Today, however, we can see more clearly what potential benefits, i.e. direct applications but also spin-offs, might be:

- Education: Basically there are two different uses for humanoids in education. (i) Students build humanoids to learn in a practical exercise about their

mechanical construction and the complex software modules that control it. (ii) Students use humanoids to experiment with and enhance their skills. The aim should be to make them very easy to use, to clearly specify their interface so as to enable non-roboticists and even students of non-engineering faculties to quickly become familiar with the robot.



Figure 1: Examples of secondary school robots

- Entertainment: Robots of human shape used for animation and advertisements at exhibitions and funfairs do not depend on a highly developed set of skills. It is usually rather their bodily appearance that attracts people because they discover human traits in these machines. To maintain a certain “surprise-factor” over time, however, it will be necessary to constantly improve their skills. Depending upon the target application, this may even include grasping and sophisticated navigation, e.g. for showing visitors around, manipulating and explaining the objects on display in a natural way.



Figure 2: Examples of entertainment robots

- Service: Unlike autonomous service robots that perform a more or less limited range of special tasks with or without human supervision, a humanoid robot can in principle use the same tools and appliances as humans and may hence become as flexible in adapting to new tasks as a human being. If it is close enough to human shape and size, it may also operate in totally unchanged man-made environments. Moreover, if it is capable of receiving its tasks by carrying on a dialogue with human instructors involving speech, gestures and facial expressions, then it will provide a functionality that surpasses by far anything that today's service robots have to offer.



Figure 3: Examples Service Robots (University of Kalsruhe's and Fujitsu's Service Robots)

- Prosthetics: If we think of the humanoid robot as a collection of prostheses for limbs but to some extent also for sensors, then it becomes clear that prosthetics and humanoid research may very fruitfully profit from each other. While there is still little evidence that cybernetic organisms ("cyborgs") may ever be realized or the human mind be transferred to these machines, prostheses that afford some autonomy of their own may become an alternative to current designs, at least until it is possible to "re-grow" human organs.



Figure 4: RoboWalker, an example of a robotic prostheses

1.2. Benchmarking

Nowadays, the emergence of humanoid robots has been extensive because of anthropomorphism, friendly design, applicability of locomotion, behaviour within the human living environments, small size and so on. In fact, one reason for its small size is safety: striding about in homes, a small robot is less likely to harm people by falling on them. Another reason is that shorter limbs and appendages are easier to move and control. To meet these demands, several humanoid robots have been developed in these years.

One of them is Qrio [Geppert, 2001], constructed by Sony. It was designed to be capable of entertaining people by interacting with them through movements and speech.

Its remarkably fluid motion comes from 38 flexible joints—4 on the neck—each controlled by a separate motor. Qrio senses its own motion through accelerometers in its torso and feet, a function similar to that of the human inner ear. It is 580 mm height and its weight is approximately 6.5Kg.



Figure 5: QRIO

Honda engineers created ASIMO [Hirose et al., 2001] that, with 26 degrees of freedom (2 on the neck, fixed eyes), can walk and perform some tasks much like a human. It is 120 cm height and weights about 52 Kg. It was the first robot able to climb stairs and run.

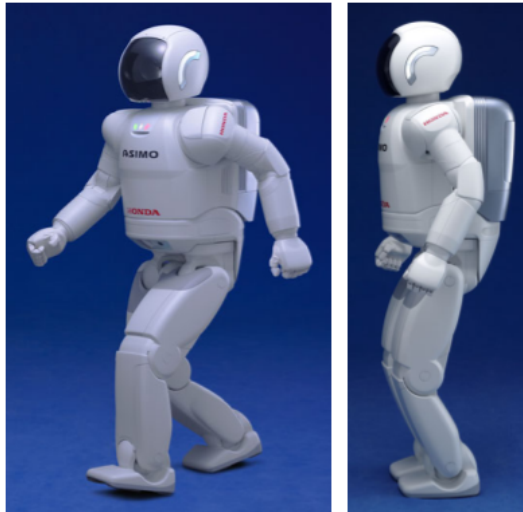


Figure 6: ASIMO

PINO project [Yamasaki et al., 2000] was started in November 1999 and its key concepts for this project were: develop platform for perception and behaviour research using multiple perception channel and high DOFs; investigate robot design that are well received by general public and develop affordable humanoid platform using off-the-shelf components and low-precision materials. The size of the robot is carefully designed to be the size of the 1.5 year-old kids (height 70cm). It has 26DOFs and 4.5 Kg of weight.



Figure 7: PINO

Another miniature humanoid robot is Fujitsu's HOAP-2 [www.automation.fujitsu.com]. This platform has been programmed to perform moves from the Chinese martial art taijiquan, as well as Japanese Sumo wrestling stances as well as to aid to robotics research. This robot's weight is less than 7 kg and its height is about 500 mm. It has a total of 25 DOFs, 2 in the neck.

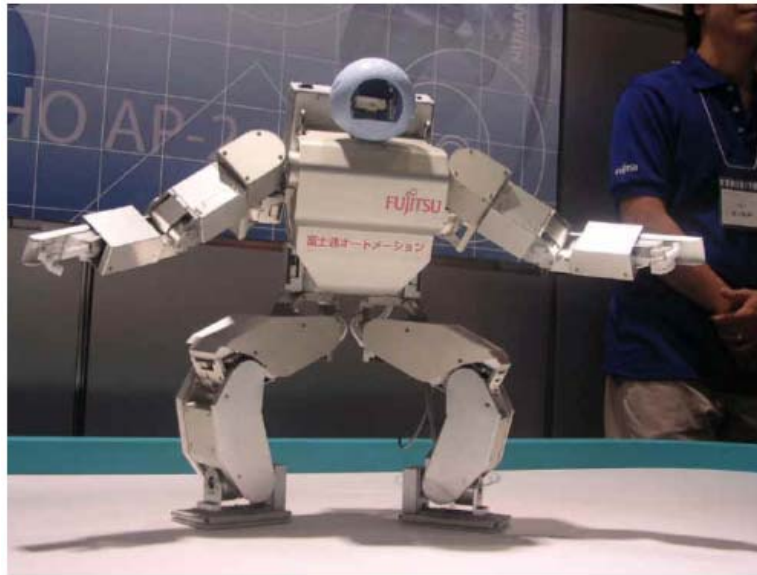


Figure 8: HOAP-2

After analysing all this well-known solutions, we could conclude that most of the existing humanoid systems have a simplified head with a small number of degrees of freedom (Table 1).

In our case, since the iCub is designed to be a tool for studying the human cognition system and as “object manipulation” plays a key role in the development of cognitive capability, the design of this humanoid robot aims to maximize the number of degrees of freedom of the upper part of the body (head, torso, arms, and hands). Given that, it was established that the iCub head should have, at least, 6 degrees of freedom (3 on the neck and 3 on the moving eyes).

Robot	Head DOF	Moving Eyes?	Eyes DOF
Qrio	4	✗	----
ASIMO	2	✗	----
PINO	2	✗	----
HOAP-2	2	✗	----
iCub	6	✓	3

Table 1: Head DOF of analyzed solutions

1.3. Our Approach

While the development of high dynamically skilled humanoid robots ([Geppert, 2001], [Hirose et al., 2001], [Yamasaki et al., 2000]) may well succeed in

traditional markets, the greatest challenge from a research perspective is the use of humanoids as subjects in Cognitive Sciences [Lopes et al., 2004].

Without doubt there is no other machine conceivable on which we may simulate more realistically the development of cognitive processes in developmental psychology, linguistics, etc. – emulating perception and action in the same world in which human beings grow up. The humanoid robot's body, if equipped with a rich set of human-like sensors, generates a stream of multimodal and multidimensional information about the environment that very closely resembles the input to the human perception system. The "motor side" also requires the control of actuators in an extremely high dimensional workspace to act in the real three dimensional world in real time, similar to what the human nervous system has to control. Research need not be limited to study individual development; one can also imagine the study of "inter-humanoid" relations in humanoid societies or the evolution of collective intelligence in such swarms of humanoids.

The ICub robotic head/neck system is included in the European Project RobotCub, a large and ambitious project of embodied cognitive systems [Sandini et al., 2004].

The RobotCub project has the twin goals of (1) creating an open and freely-available humanoid platform, iCub, for research in embodied cognition, and (2) advancing our understanding of cognitive systems by exploiting this platform in the study of cognitive development. To achieve this goal we plan to construct an embodied system able to learn: i) how to interact with the environment by complex manipulation and through gesture production & interpretation; and ii) how to develop its perceptual, motor and communication capabilities for the purpose of performing goal-directed manipulation tasks. iCub will have a physical size and form, similar to that of a two year-old child and will achieve its cognitive capabilities through artificial ontogenic codevelopment with its environment: by interactive exploration, manipulation, imitation, and gestural communication.

The iCub will be a freely available open system which can be used by scientists in all cognate disciplines from developmental psychology to epigenetic robotics. It will be open both in software but more importantly in all aspects of the hardware and mechanical design.

One of the tenets of the RobotCub stance on cognition is that manipulation plays a key role in the development of cognitive capability. Consequently, the design is

aimed at maximizing the number of degrees of freedom of the upper part of the body (head, torso, arms, and hands).

The iCub will have head, torso, two arms/hands and two legs. The legs will be used for crawling but, possibly, not for biped walking. This will allow the system to explore the environment not only by manipulating objects but also through locomotion. For this reason, it is particularly important to equip the iCUB with enough degrees of freedom to allow transition between sitting and crawling posture, as well as to look down while manipulating objects lying on the floor. The iCub is about 90cm tall, weighs 23 kg and has a total of 53 degrees of freedom organized as follows: 7 for each arm, 8 for each hand, 6 for the head, 3 for the torso/spine and 7 for each leg.

The mechanics, electronics and software components of the iCub are being developed by the RobotCub's team in parallel and synergistically. Concerning the mechanical hardware, the legs and spine were developed by University of Salford, UK, the arms and hands were developed by University of Pisa, Italy and the head was developed by us, in IST, Portugal.

The eye-head sub-system will include basic visual processing primitives, as well as low-level oculomotor control, visual, inertial and proprioceptive sensors. The iCub will have two arms with the motor skills and sensory components required for dexterous manipulation. From the control point of view, reaching and grasping primitives will be implemented together with primitives to acquire tactile and proprioceptive information. It is expected that most of the actuators of the hand will be located in the forearm. The hands will be underactuated. This is implemented by means of mechanical coupling either rigidly, such as using a single tendon to bend two joints of a finger alike, or by an elastic coupling of the joints. Underactuation also saves on space, power consumption, and cost.

As we can see, most of the existing humanoid systems have a simplified head with a small number of degrees of freedom. In our case the interaction with other robots or individuals is very important, justifying the need to include a larger kinematic complexity, while meeting very stringent design constraints, in terms of weight and size.

1.4 Thesis Organization

This thesis is organized in the following manner:

- Chapter 1 introduces the research context in which the work was developed together with the description of the general objectives.
- Chapter 2 provides the project specifications, based on biological, anatomical and behavioral data, as well as tasks constraints.
- Chapter 3 presents the model development, including concepts generation, the mechanical design, actuators selection and analysis made during the design process, as well as, all assumptions made regarding the assembly and protection of the mechanical system.
- Chapter 4 briefly shows the tests that were made after the production of the working prototype, in order to check its mechanical performances.
- Chapter 5 gives the final conclusions.

2. Head Specifications

In this section we summarize some of the human anatomic and behavioral data, considered in the head design and the assumptions that were made to get the specifications of this particular robot.

2.1. Anatomical Data

1) Neck: The human neck has a very complex muscular and skeletal system, with more than twenty muscles and ten bones [Netter, 1998]. The head has more complexity if we consider the mouth, the eyes and the facial expressions.

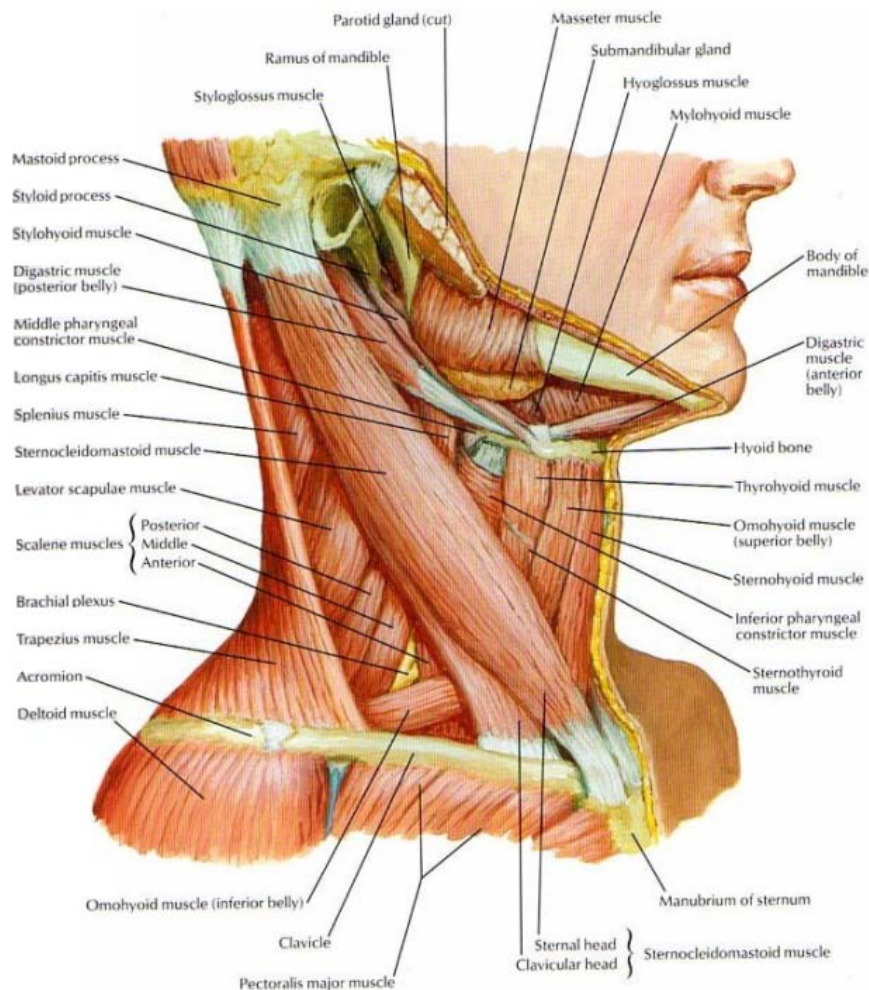


Figure 9: Human Neck muscular system [Netter, 1998]

The neck is constituted by seven vertebrae and the atlas that supports the skull.

The vertebrae can be considered a flexible spring giving flexion/extension and adduction/abduction motion. The atlas bone gives the possibility of rotating the head and an upper flexion/extension movement. All these bones are actuated by muscles in a differential way. For every motion agonistic and antagonistic muscles are used, having each of them a flexion, rotation and abduction function, e.g. consider the sternocleidomastoid muscle. Some of the muscles begin in the spine, e.g. the trapezoidal, and continue through in the neck.

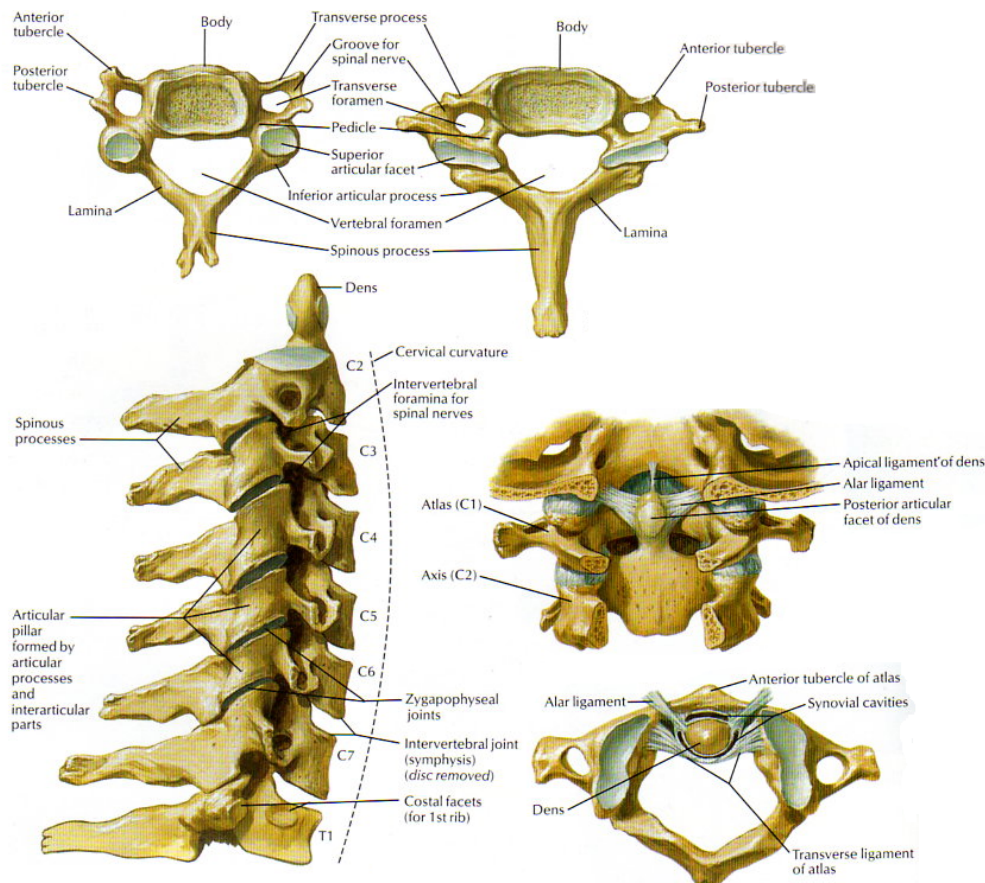


Figure 10: Human Neck skeletal system [Netter, 1998]

The neck kinematic model has been the object of studies in human biomechanics, for the analysis of injuries caused by impacts, sports training, etc. The most standard model of the human neck has four degrees of freedom ([Silva, 2003], [Laananen, 1999], [Zatsiorsky, 1997]).

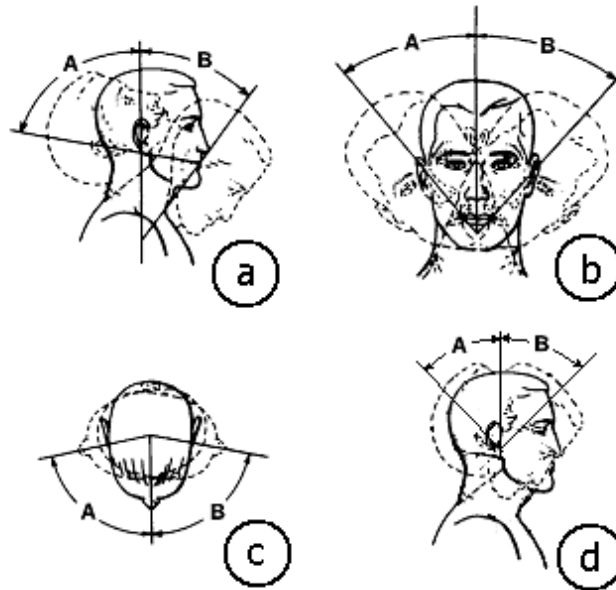


Figure 11: Standard human neck 4 DOF; a) Neck Flexion, A, and Extension, B; b) Neck Lateral Bend Right, A, and Left, B; c) Neck Rotation Right, A, and Left, B; d) Atlanto-occipital Flexion, A, and Extension, B;

2) Eyes: Each human eye has six muscles. As it is a globe inside a socket three motions can be considered, abduction/ adduction, elevation/depression and rotation [Netter, 1998]. The muscles have combined actions to achieve these motions, as described in Figure 12 and Table 2. Note that each eye is completely independent of the other.

Muscle	Action
Superior rectus	Elevates, adducts, and rotates eyeball medially
Inferior rectus	Depresses, adducts, and rotates eyeball laterally
Lateral rectus	Abducts eyeball
Medial rectus	Adducts eyeball
Superior oblique	Abducts, depresses, and medially rotates eyeball
Inferior oblique	Abducts, elevates, and laterally rotates eyeball

Table 2: Eye Muscles Actuation [www.eyegk.com]

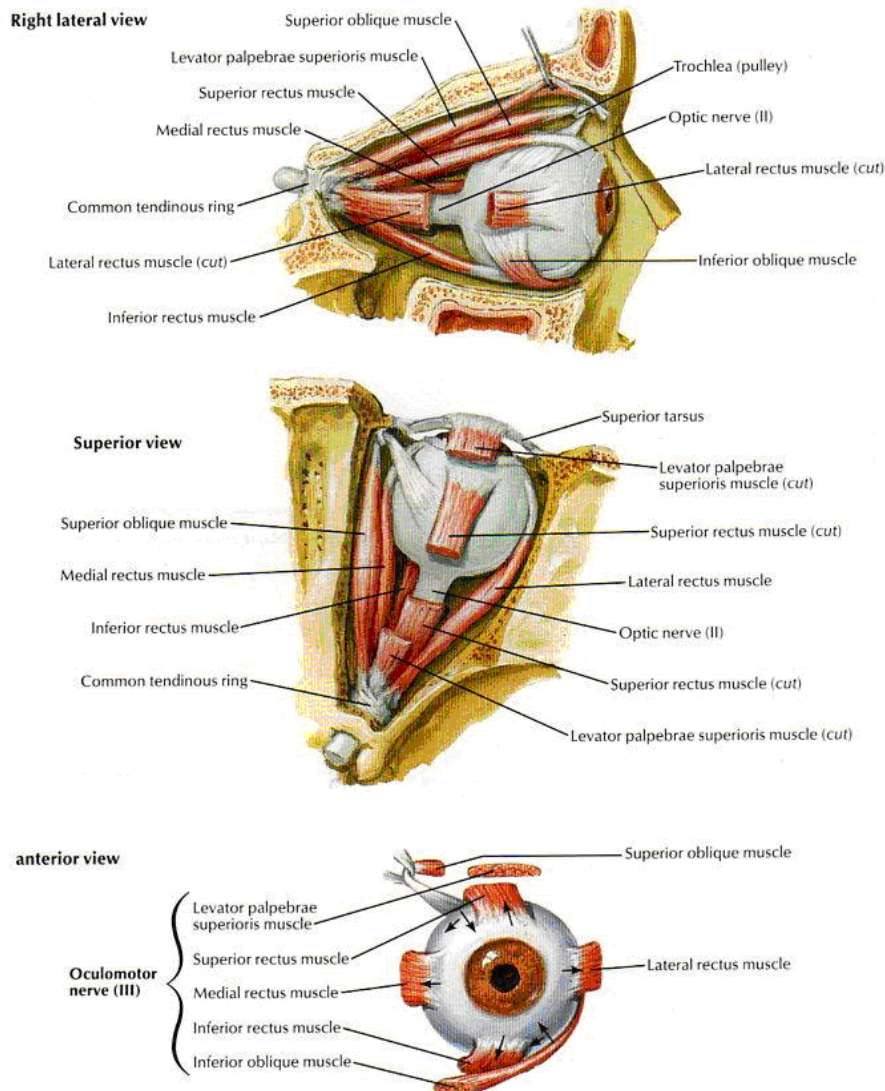


Figure 12: Eye Muscles Actuation [Netter, 1998]

The human oculomotor system combines several basic movements: saccades, smooth pursuit, vergence, vestibuloocular reflex, optokinetic reflex, microsaccades and accommodation.

The saccadic and smooth pursuit eye movements occur when the eyes pursue an object. During smooth pursuit, the eye tries to match the (angular) speed of the tracked target, usually at relatively low speeds (up to 30°/s). The saccadic eye movement occurs when the eye ball movement is not able to pursue an object or when the human searches outside of the view. It is composed by high speed jumping movements, in the range of a few hundreds degrees per second.

Figure 13 shows some typical patterns of gaze movements, composed by an initial eye-in-orbit saccade onto the target (the peak periods of velocity and acceleration

patterns) followed by a synkinetic and much slower head movement. The vestibular ocular reflex generated by head acceleration drives the compensatory eye movement, eye-in-orbit, in the opposite direction so that gaze, eye-in-space remains on target.

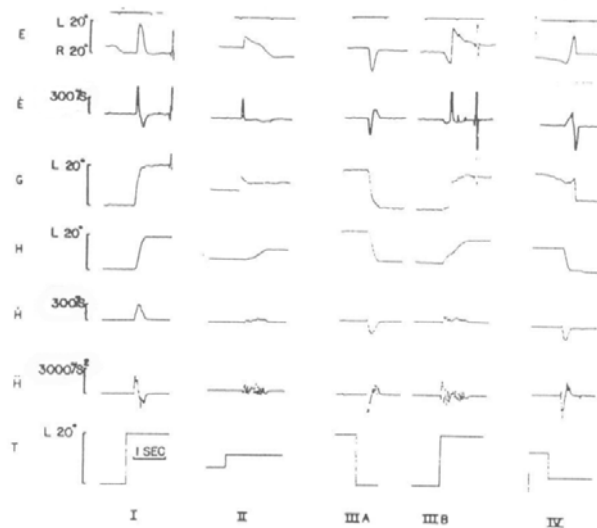


Figure 13: Coordinated gaze types. Eye position (E), eye velocity (E'), gaze position (G), head position (H), head velocity (H'), and acceleration (H''), and target position (T). 40° movements between left (L) and right (R).

[Zangemeister et al., 1981]

In Figure 14 we can find the eye/neck speed for human adults during saccadic movements with 2.5, 5, 10, 40 and 60 degrees of amplitude.

	E	H	E	H	E	H	E	H	E	H
Magnitude (degrees)	2.5	2.5	5.0	5.0	10.0	10.0	40.0	40.0	60.0	60.0
Duration (msec)	24.5	260	28.5	270	37	300	78	320	110	380
v_{max} (deg/sec)	166	22.5	320	48	519	80	791	270	850	352
t_{vmax} (msec)	—	90	—	95	—	105	—	125	—	125
a_{max} (deg/sec ²)	16000	330	28000	551	41000	994	73000	2100	82000	3300
a_{min} (deg/sec ²)	—	322	—	392	—	714	—	1850	—	2700

Figure 14: Main Sequence Data for Eye (E) and Head (H)

[Zangemeister et al., 1981]

The saccade speed increases with the motion amplitude. Hence, the speeds during small amplitude saccades resemble those of smooth pursuit. These data also show how the effort is divided amongst eye and neck degrees of freedom when some redundancy exists (e.g. eye and neck pan movements). This information will be used for the design of the iCub specifications.

Table 3 presents relevant data from Figure 14.

Adult values Head Weight: 4.5-5Kg		Velocity		Acceleration	
		[°/s]		[°/s²]	
		min	max	min	max
Eyes	pan	166	850	16000	82000
	tilt				
Neck	pan	23	352	330	3300
	tilt				
	swing/roll				
Neck/Eye (pan) ratio		14%	41%	2%	4%

Table 3: Anthropomorphic data ([Panero et al., 1979], [Zangemeister et al., 1981]), showing the motion amplitude and speed for some degrees of freedom in the human eye/neck system

2.2. Robot Head Specifications

The initial specifications for the iCub are quite demanding, both per size (Figure 15) and weight. The total head weight should not exceed 2 Kg and the size is that of a 2 year old child. The head is 13.6 cm wide, 17cm long and 17.3cm deep. The neck is 7cm wide and 9cm long. For modularity, we divide the head in the neck and eye subsystems.

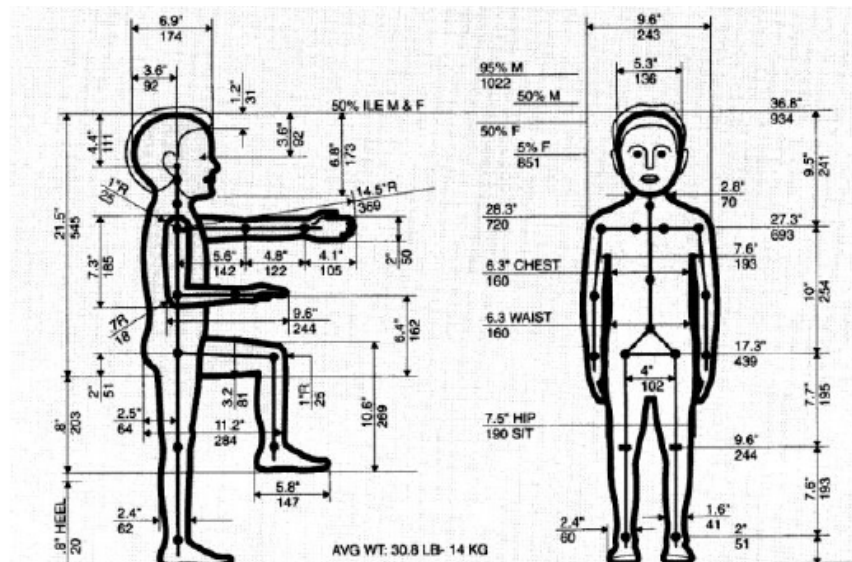


Figure 15: Approximate size targeted for the iCUB [Tilley, 2001]

In order to guarantee a good representation of the human movements, the iCub head contains a total of 6 DOFs: neck pan, tilt and swing, and eye pan (independent) and tilt (common) as shown in Figure 16. The neck tilt and swing motion axes intersect the neck pan's and the eye pan axes intersect the eye tilt's.

A minimal set of facial expressions were used (implying the smallest possible number of motors or moving parts) to convey information about the robot's emotional status.

Although the human neck has four dof, as the space/weight limitations are very large the neck was modeled with three degrees of freedom. The atlanto-occipital flexion/extension was ignored. For most tasks this motion is not necessary, since orienting the eyes towards a scene point is essentially a two degree of freedom task. Therefore, the neck still has some redundancy that can be used to avoid obstacles, occluders or to choose better viewpoints.

The eyes cyclotorsion was ignored because it is not useful for control, and similar image rotations are easily produced by software. The elevation/depression from both eyes is always the same in humans, in spite of the existence of independent muscles. Similarly, a single actuator is used for the robot eyes elevation (tilt). Eye vergence is ensured by independent motors. Figure 12 shows the final chosen kinematics, that allows all basic ocular movements.

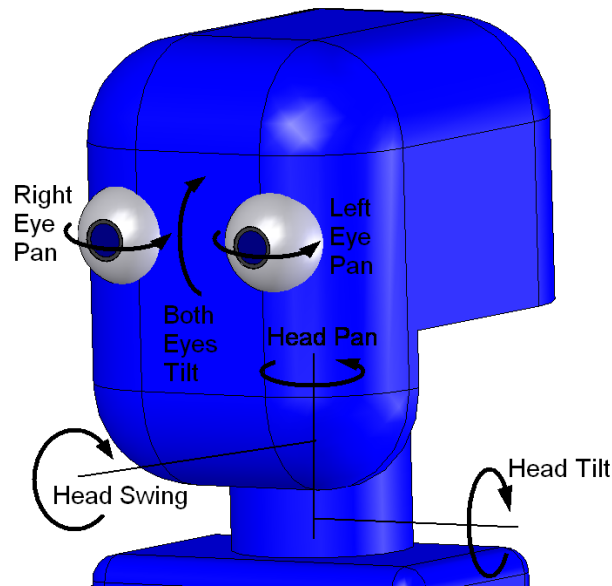


Figure 16: Illustration of the Head degrees of freedom. There is a total of six degrees of freedom, three for the neck and three for the eye system (facial expressions are not included)

One of the most critical design steps is that of defining the desired velocities and accelerations for the various head joints. This will directly impact on the choice of motors and therefore on size/weight constraints.

Data regarding accelerations, velocities and joint range of the oculomotor system of human babies are not available, and very few studies exist in the literature of psychology or physiology. This section explains how we obtained the anthropomorphic data and specifications for the iCub robot head. Overall, the iCub dimensions are those of a two-year-old human child, and it is supposed to perform tasks similar to those performed by human children.

In Table 2 there are two key observations for the iCub head design. First, we used the smaller range of saccadic speeds as a reference, since (i) these are adult data and children have significantly smaller speeds and (ii) small amplitude saccades are close to smooth pursuit movements, which are far more frequent during the robots normal operation. Secondly, we used the ratio between neck/eye velocity (14% - 41%) and acceleration (2% - 4%) as an important design parameter.

Using this information, and hypothesizing a trapezoidal motion profile (Figure 17) for the eye movements (as axes control boards usually specify), we can compute the necessary joint acceleration.

The typical motion controller calculates the motion profile trajectory segments based on the programmed parameter values. The motion controller uses the desired target position, maximum target velocity, and acceleration values to

determine how much time it spends in the three move segments (which include acceleration, constant velocity, and deceleration).

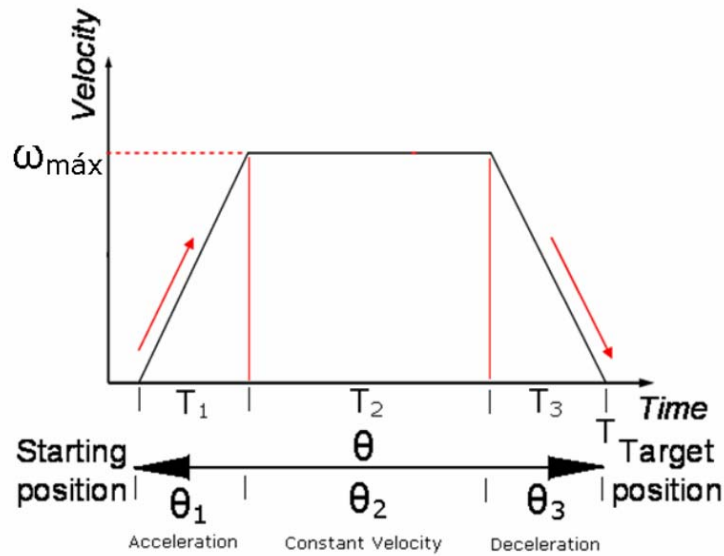


Figure 17: A typical trapezoidal velocity profile

For the acceleration segment of a typical trapezoidal profile, motion begins from a stopped position or previous move and follows a prescribed acceleration ramp until the speed reaches the target velocity for the move.

Motion continues at the target velocity for a prescribed period until the controller determines that it is time to begin the deceleration segment and slows the motion to a stop exactly at the desired target position.

The acceleration, a , can be calculated as a function of the total time of the movement, T , the total range of the movement for each joint, θ , and the ratio between the total time of the movement and the acceleration/deceleration time (T_a), f .

From Figure 17, we have:

$$T = T_1 + T_2 + T_3 \quad \text{and} \quad \theta = \theta_1 + \theta_2 + \theta_3 \quad (1) \text{ and } (2)$$

Considering T_a to be acceleration/deceleration time, we get:

$$T_a = T_1 = T_3 = f \cdot T \quad (3)$$

In acceleration/deceleration periods, the movement range, θ_a can be calculated as:

$$\theta_a = \frac{1}{2} \cdot \alpha \cdot T_a^2 = \frac{1}{2} \cdot \alpha \cdot f^2 \cdot T^2 \quad (4)$$

During the moment where ω is constant, and performing its maximum value, we have:

$$\omega_{\max} = \frac{\theta_2}{T_2} \quad (5)$$

and

$$\omega_{\max} = \alpha \cdot T_a = \frac{\theta_2}{T_2} \quad (6)$$

Using this on equation 2, we get:

$$\alpha = \frac{\theta}{f \cdot T^2 \cdot (1 - f)} \quad (7)$$

For that purpose we only need to define the percentage of time that corresponds to acceleration/deceleration (e.g. $f = 0.2$), while the remaining part of the trajectory is executed at maximum speed. Table 4 shows the final specifications.

The design parameters used indicate that the ratio between neck/eye velocities is 50%, clearly above human data. We further assume that 20% of the time is used for acceleration (and another 20%) for slowing down. Although the neck swing is usually slower than other neck DOFs, we considered the ratio between neck swing/{tilt, pan } velocities to be unity. Finally, we postulated that the eye pan maximum velocity would be 180°/s. The specifications were used for the remaining part of the design.

		Range [°]	Vel Max [°/s]	Acceleration full range		
				ac.[°/s ²]	T [s]	mean vel
Eyes	pan	90	180.0	1440	0.625	144
	tilt	80	160.0	1280	0.625	128
Neck	pan	110	90.0	295	1.528	72
	tilt	90	73.6	241	1.528	59
	swing/roll	80	65.5	214	1.528	52

Table 4: Computed set of angular speed and acceleration for the various degrees of freedom of the Robot Cub Head

3. Model Development

The development of a humanoid robot within the scope of special research area has the objective of creating a machine that closely cooperates with humans. This leads to requirements such as little weight, small moving masses (no potential danger for persons in case of collision), as well as appearance, motion space, and work movements after the human model. One reason for the last point is the requirement for the robot to operate in surroundings designed for humans. Another aspect is the acceptance by technologically unskilled users, which is likely to be higher if the robot has a humanoid shape and calculable movements.

A humanoid robot is a highly complex mechatronic system, as the required functionality can only be achieved by the interplay of mechanical components with extensive sensor technology, modern actuators and highly developed software.

Successful development of complex mechatronical systems is only possible in close cooperation of specialists of the concerned fields of mechanics, electronics, and information technology. Discipline-oriented partial solutions cannot provide or only with significant delays the desired result.

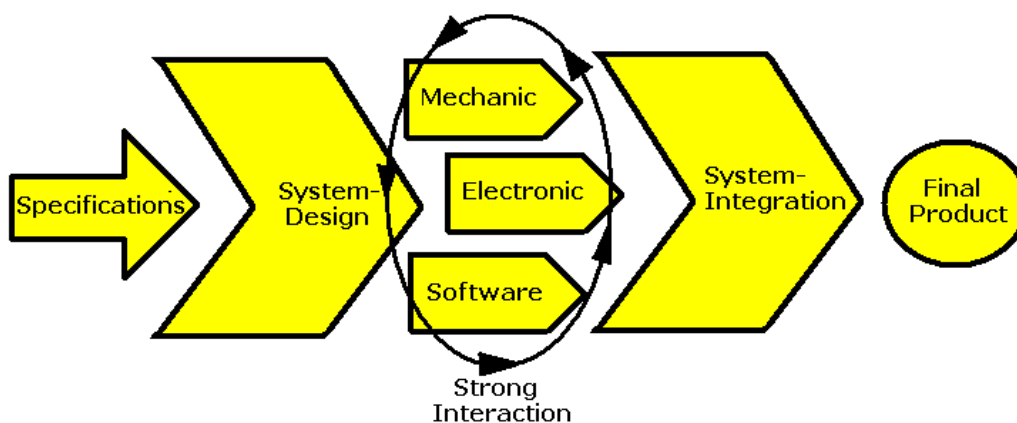


Fig. 18: Product development process in Robotics

As mentioned in the previous sections, the design concepts of the RobotCub Head are light, compact, but performable for its working applications, meeting the project dynamic and kinematics specifications. To realize this robot head, several distinctive mechanisms were employed, produced in different materials and actuated by diverse types of actuators. In this section, the details of mechanical design are introduced.

The Mechanical Design of the iCub head is divided in three major subsystems: Neck Mechanism, Eyes Mechanism and Cover (face) for increased modularity. During the design process, we used the specifications derived previously and adopted the following desirable characteristics/criteria:

- DOFs, range of motion, joint speed and torque according to detailed specifications,
- Compactness and weight, to meet all the desired specifications (< 2 Kg),
- Modularity and simplicity of the structure to facilitate maintenance and assembly,
- Self-contained to facilitate integration with the other parts of the robot,
- Robustness, to resist the efforts suffered during its working period,
- Use of standard mechanical components.

The following sections describe the various possibilities considered for each component.

3.1. Neck Mechanism

For the Neck Mechanism, 3 different solutions were considered (Figure 19).

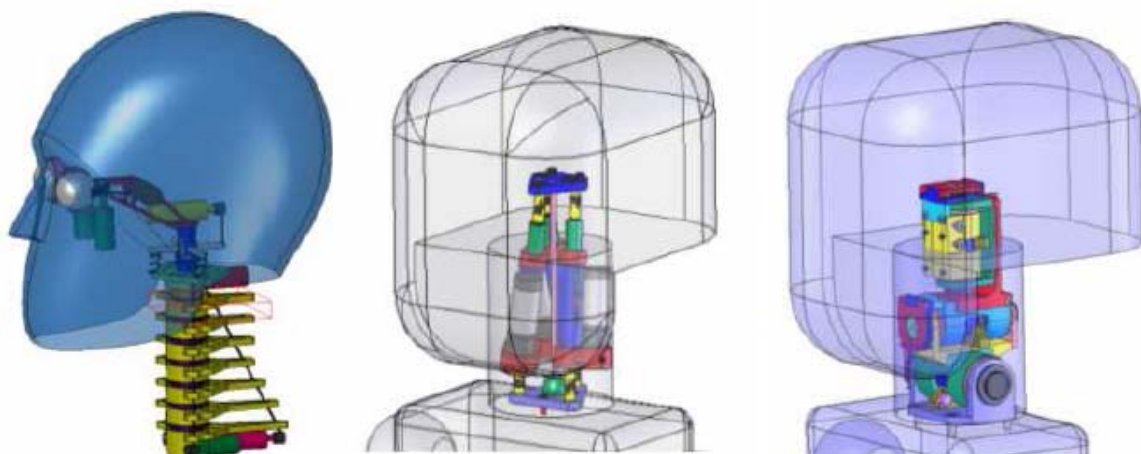


Figure 19: Three alternative solutions for neck mechanism

3.1.1. Flexible Neck Solution

Inspired by the flexibility of human neck, one design concept included a flexible neck, which would work as a spring (represented by the red cylinder), Figure 20, actuated with 3 cables separated 120° apart, producing a spherical motion of the head. A final motor could be included on top, assuming the function of atlas, for the head pan.

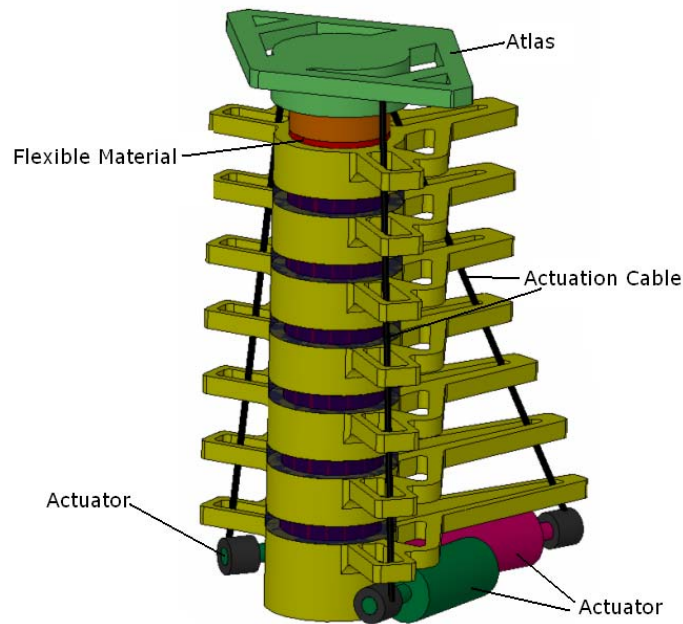


Figure 20: Prototype of robot head with spring-based neck.

Flexible-link robotic manipulators have many advantages with respect to conventional rigid robots. These mechanisms are built using lighter and cheaper materials, which improve the payload to arm weight ratio, thus resulting in an increase of the speed with lower energy consumption. Moreover these lightweight arms are more safely operated due to the reduced inertia and compliant structure, which is very convenient for delicate assembly tasks and interaction with fragile objects, including human beings.

However, the dynamic analysis and control of flexible-link manipulators is much more complex than the analysis and control of the equivalent rigid manipulators. From the modeling standpoint, the challenges are associated with the fact that the non-linear rigid body motions are now strongly coupled with the distributed effects of the flexibility along the mechanical structure. This coupling varies with the system configuration and the load inertia. Besides, the dynamic equations of flexible structures are infinite dimensional, although for control purposes

approximated finite order models are usually considered. This truncation, along with the difficulties in modeling the coupling and nonlinearities of the system, can be the source of uncertainties in dynamical models, which in turn can lead to poor or unstable control performance.

Conventional rigid-link manipulators are modeled as a set of nonlinear coupled ordinary differential equations (ODEs). However, in the case of flexible manipulators this rigid dynamics is coupled with the distributed effects of the flexibility along the mechanical structure, which lead to a model expressed in partial differential equations (PDEs), where both time and spatial derivatives are relevant. PDEs are not very convenient as models for control design purposes, since they are theoretically equivalent to infinite-dimensional systems.

To perform the system control of this kind of solution we would have to adapt a more inconvenient approach. Namely, we would need a sensor structure to apply feedback onto the system, in order to achieve a close-loop control (Figure 21). So, an inertial sensor should be included, giving us continuously information about the head position.

A similar design, using a spring as a neck, was produced by our partners on the University of Genoa (Figure 22).

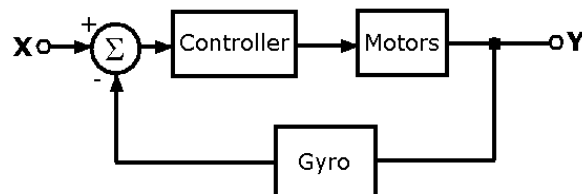


Figure 21: Feedback control system



Figure 22: Prototype of robot head with spring-based neck, produced by University of Genoa

Another problem with this design, further than control complexity, is that motors would have to be placed in the robot chest, jeopardizing the design modularity. Given that, this solution was discarded.

3.1.2. Parallel Mechanism Solution

To be modular and self-contained, the head structure must support a large number of mechanical and electrical components. On the other hand, high torque motors are required to drive the cameras, in particular to achieve the velocity of saccadic eye movements. So, to satisfy both (conflicting) requirements, an interesting solution for the robot neck structure is based on a parallel mechanism (Figure 22).

Parallel mechanisms have remarkable characteristics such as high precision, high load capacity, high rigidity, interior space for cabling and easy solutions for the inverse kinematics. Also, since all motors are fixed on the base, the inertia of the moving part is relatively small.

There are several categories of parallel mechanisms, and their classification is made fundamentally according to their degrees of freedom, motion type and geometrical architecture [Merlet, 2001]. In our case, since we were trying to reproduce the movement of a 3 dof rotational neck, the most suitable solutions were on the special 3 dof orientation mechanisms (Figure 23).

Three dof orientation mechanisms allow three rotations about one point and represent an interesting alternative to the wrist with three revolute joints having convergent axes classically used for serial robots.

In order to provide only rotary motions about one point, one can use four generators. One of them being a passive generator of rotary motion about one point.

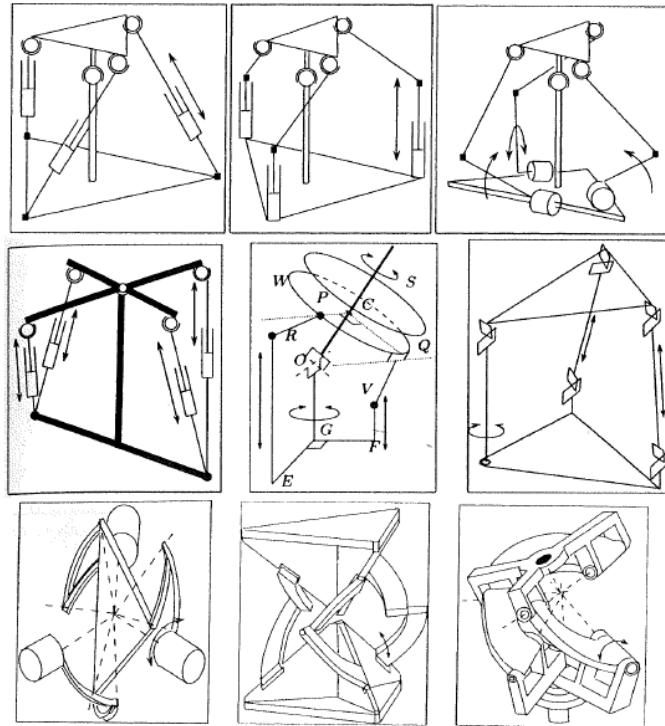


Figure 23: Various architectures of three dof orientation mechanisms [Merlet, 2001]

The simplest, and chosen solution, was the 3-UPS architecture (Figure 24), where each generator active link is composed by an universal joint, a prismatic joint and a spherical joint.

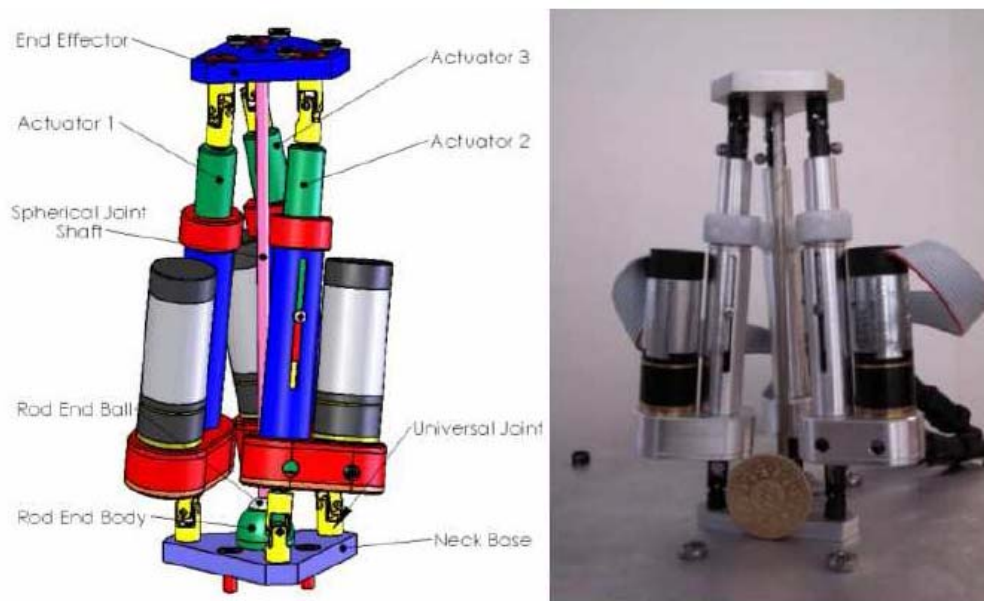


Figure 24: CAD Model of the Parallel Neck and prototype

Because of its complex 3D geometry, the design of the 3-UPS solution is not very trivial. Therefore, the calculation of the actuator's stroke, required maximum velocity and load capacity were made using Kinematic and dynamic simulations.

The kinematic modeling of the 3-UPS architecture, [Gregorio, 2003], [Alici et al., 2004], [Gregorio, 2004], was made considering it to be composed of a fixed tetrahedron, a moving tetrahedron and three identical limbs (Figure 25). The tetrahedrons have equilateral triangular bases of different sizes. The tips of the tetrahedrons are linked using a spherical joint. The limbs are connected to the moving tetrahedron base with 2-DOF universal joints and to the fixed tetrahedron base with spherical joints. A linear actuator controls the leg length, and forms a prismatic joint. Each universal joint is treated as two revolute joints with axes perpendicular to each other and intersecting at a point.

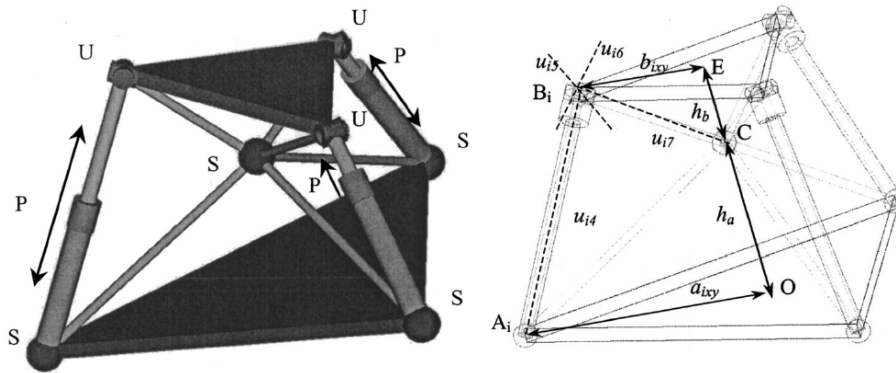


Figure 25: Parallel Mechanism Architecture [Alici et al., 2004].

In Figure 23, u_{i4} is the unit vector along the prismatic joint axis for leg i , u_{i5} and u_{i6} are the unit vectors along the axes of the universal joint of leg i . u_{i7} is the CB_i edge of the moving tetrahedron [Alici et al., 2004].

A coordinate system is chosen for each tetrahedron as shown in Figure 26. Frames A and B are defined for the base and moving tetrahedrons respectively. Their origin is placed at the common tip of the tetrahedrons and represents the point around which the moving tetrahedron rotates.

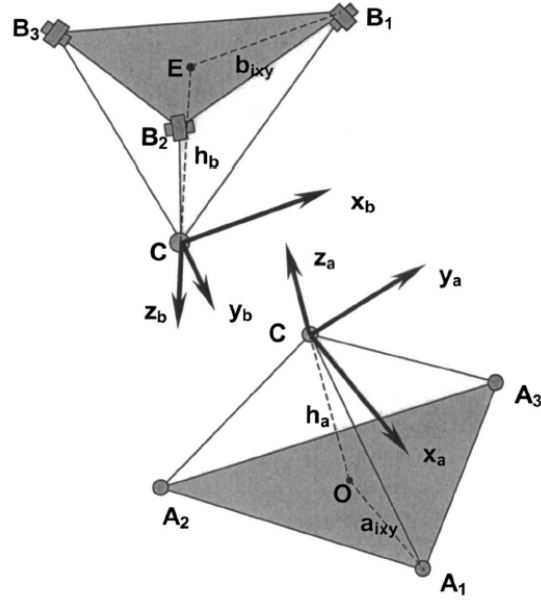


Figure 26: Coordinate systems of the 3-UPS platform.

As seen in Figure 26, the position vectors of points A_i and B_i with respect to frames A and B respectively, can be written as:

$${}^A a_i = [a_{ix}, a_{iy}, -h_a]^T, \quad \text{and} \quad {}^B b_i = [b_{ix}, b_{iy}, -h_b]^T \quad (8)$$

The scalar a_{ixy} , shown in Figure 26, denotes the distance between the center, O, of the base triangle of the fixed tetrahedron and anyone of the corners of the base triangle. The scalar b_{ixy} denotes the distance between the center, E, of the base triangle of the moving tetrahedron and any of the corners of the base triangle. The parameter c_i denotes the difference between a_{ixy} and b_{ixy} .

Parameter d_i denotes the length of leg i . The vector d_i represents the position vector of the leg i ($A_i B_i$) in the base coordinate system:

$${}^A d_i = [d_{i,xa}, d_{i,ya}, d_{i,za}]^T \quad (9)$$

The scalar h_a denotes the height of the fixed tetrahedron and is the distance from point O to point C. The scalar h_b denotes the height of the moving tetrahedron and is the distance from point E to point C. The parameter h represents the total height of the parallel platform in (0,0,0) orientation and is equal to the sum of h_a and h_b . The parameter h_{ab} is the ratio between h_a and h_b .

The transformation from the moving frame B to the fixed frame A can be described by a 3x3 rotation matrix ${}^A R_B$ defined by a z-x-z (φ - θ - ψ) Euler rotation. Given that, in the initial position (0-0-0 rotation) the x_a and x_b axes coincide, z_a and z_b , and y_a and y_b are in opposite directions respectively, the resulting rotation matrix is given by:

$${}^A R_B = \begin{bmatrix} c\phi c\psi - s\phi c\theta s\psi & c\phi s\psi + s\phi c\theta c\psi & -s\phi s\theta \\ s\phi c\psi + c\phi c\theta s\psi & s\phi s\psi - c\phi c\theta c\psi & c\phi s\theta \\ s\theta s\psi & -s\theta c\psi & -c\theta \end{bmatrix} \quad (10)$$

where c represents the cosine and s the sine of the following angle.

For the direct kinematics the leg lengths d_i and the triangular bases' geometry are known. The three orientation angles of the moving platform are determined from expanding the following three scalar equations:

$$d_i^2 = a_i^2 + b_i^2 - 2a_i^T b_i, \quad \text{for } i = 1, 2, 3 \quad (11)$$

For the inverse kinematics the orientation of the moving platform is known and the limb lengths, d_i are calculated from the following three equations:

$$d_i = \pm \sqrt{a_i^2 + b_i^2 - 2a_i^T b_i}, \quad \text{for } i = 1, 2, 3 \quad (12)$$

The manipulator Jacobian matrix J relates the end-effector velocities vector v to the actuated joint velocities vector \dot{d} :

$$J_x \omega + J_d \dot{d}, \quad J = J_d^{-1} J_x \quad (13)$$

For the 3-UPS platform J_x and J_d are given by:

$$J_x = \begin{bmatrix} (u_{1,7} \times u_{1,4})^T \\ (u_{2,7} \times u_{2,4})^T \\ (u_{3,7} \times u_{3,4})^T \end{bmatrix} \quad J_d = [I] \quad (14)$$

For such a small size neck (9cm x 7cm), we had to design our own linear actuators, with the mechanism moved by three Linear Ball Screw Actuators.

Comparing with other solutions, this type of actuators offers a good compromise between size, controllability and load capacity. The mechanical structure of these components is shown in Figure 27.

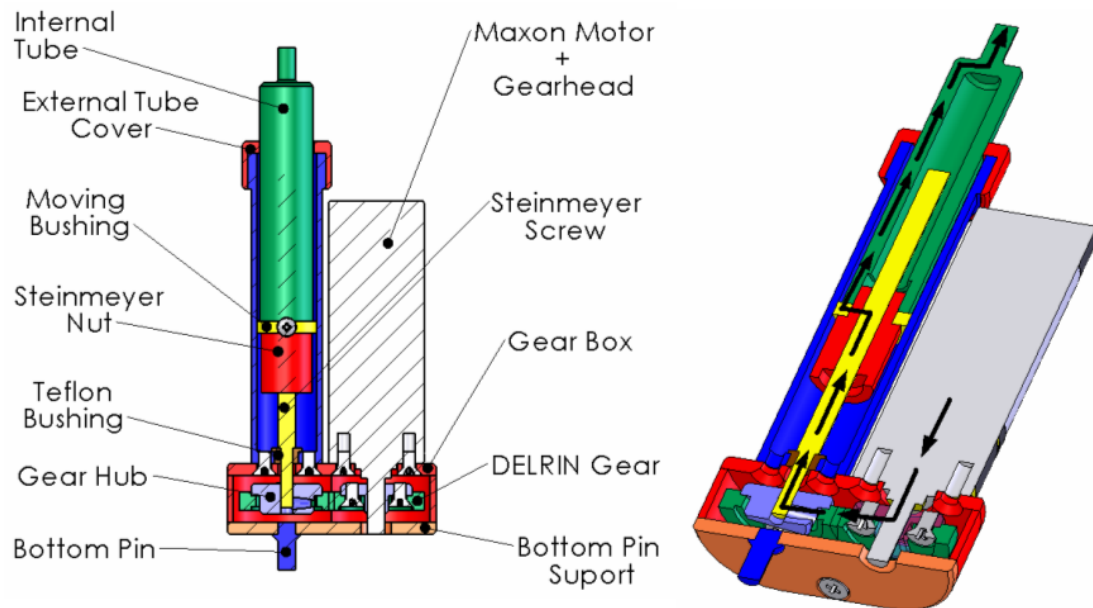


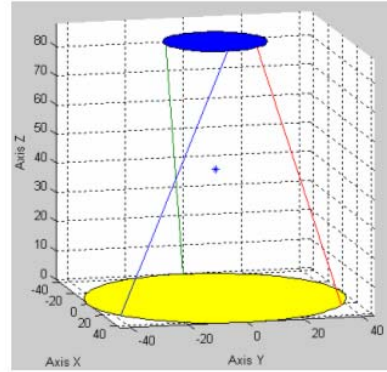
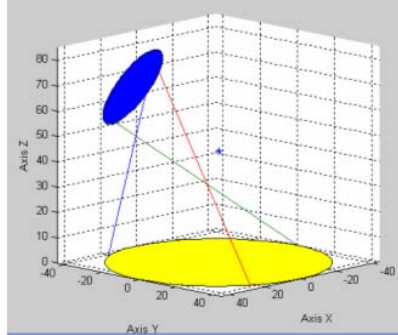
Figure 27: Ball Screw Linear actuator

This Linear Actuators have a Thomson Saginaw Configuration, which consists of a DC motor mounted parallel to a ballscrew system through a reduction gear assembly in such a way that the rotational motion produced by the DC motor produces the linear movement of the ballscrew.

So, in order to calculate the design parameters of the linear actuators (the maximum stroke, the maximum velocity and the load capacity of the actuators) several kinematic and dynamic simulations were made, in *Matlab*, and *CosmosWorks*, Figures 28 and 29.

Input:

- Dimensions
- Velocities and Accelerations
- Range of Movements



Output:

- Actuators maximum stroke = 40mm
- Actuators velocity = 60 mm/s

Figure 28: Kinematic Simulations, using *Matlab*

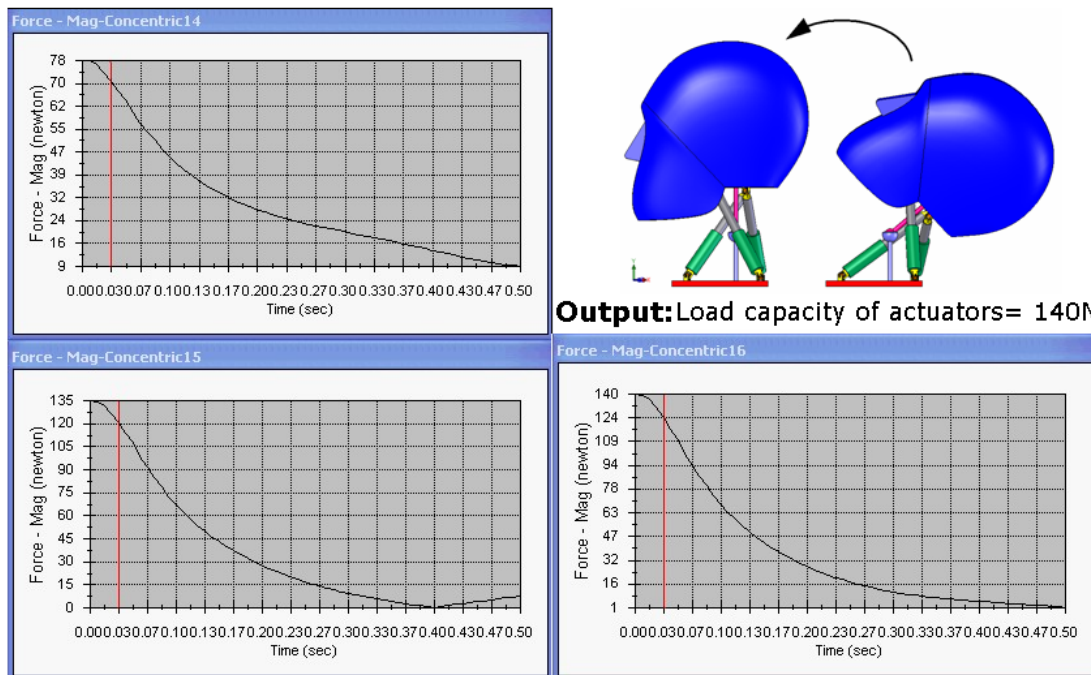


Figure 29: Dynamic Simulations, using *CosmosWorks*. The three different graphics show the evolution of the forces required in each actuator of the mechanism in maximum acceleration simulation.

The most considerable disadvantage for this concept is that it is very difficult to avoid the interference between the various parts, for such large movements, decreasing significantly its workspace. Given that, this solution was also discarded.

3.1.3. Serial Mechanism Solution

The third tested solution was of a serial manipulator with three degrees of freedom, placed in a configuration that best represents human neck movements. In spite of its simplicity, the mechanism is very robust, easy to control and highly performing, meeting all the specifications. For these reasons, this was the final choice adopted for the iCub head neck.

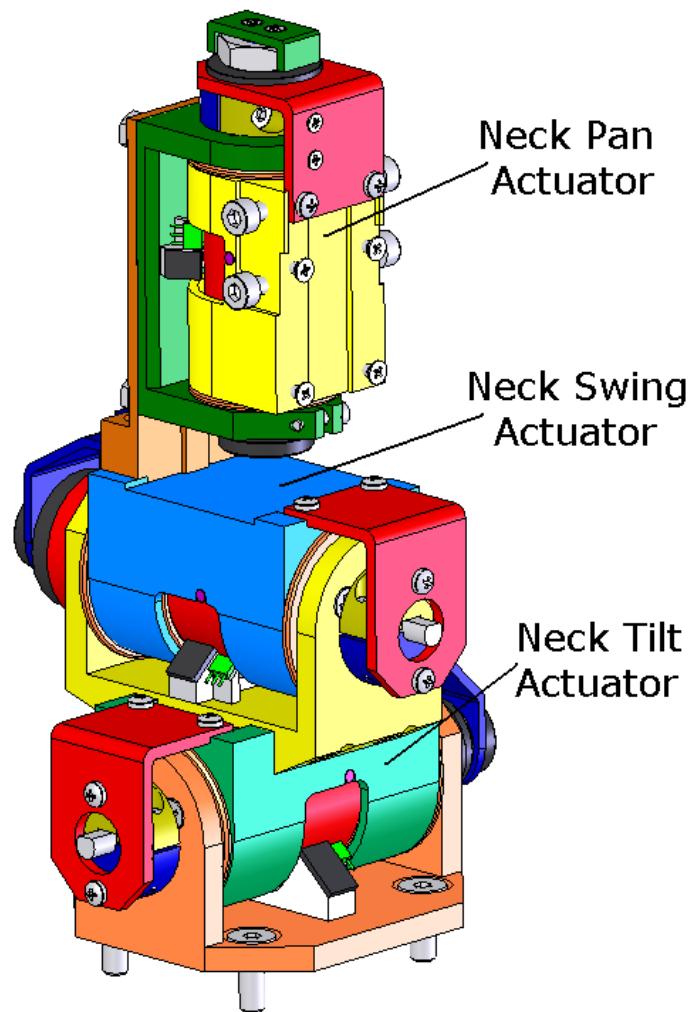


Figure 30: CAD Model of Serial Mechanism

As can be seen in Figure 30, the neck mechanism is a serial manipulator composed by 3 revolution joints. The tilt joint is the first one, followed by the swing joint and the pan joint, whose axis of rotation crosses the other two. To realize them, a compact design for mechanism that is composed by 3 different actuation modules, for the 3 different joints was employed. Figure 31 shows an element of compact

design and the drive system mechanism, used in all joint of the neck. Its mechanism is formed from DC motor (together with a respective gearbox and encoder), rotational bushings, mechanical stop, and an absolute position sensor. This setup can be considered very robust since the axial and radial external loads are not transmitted to the actuator's shaft.

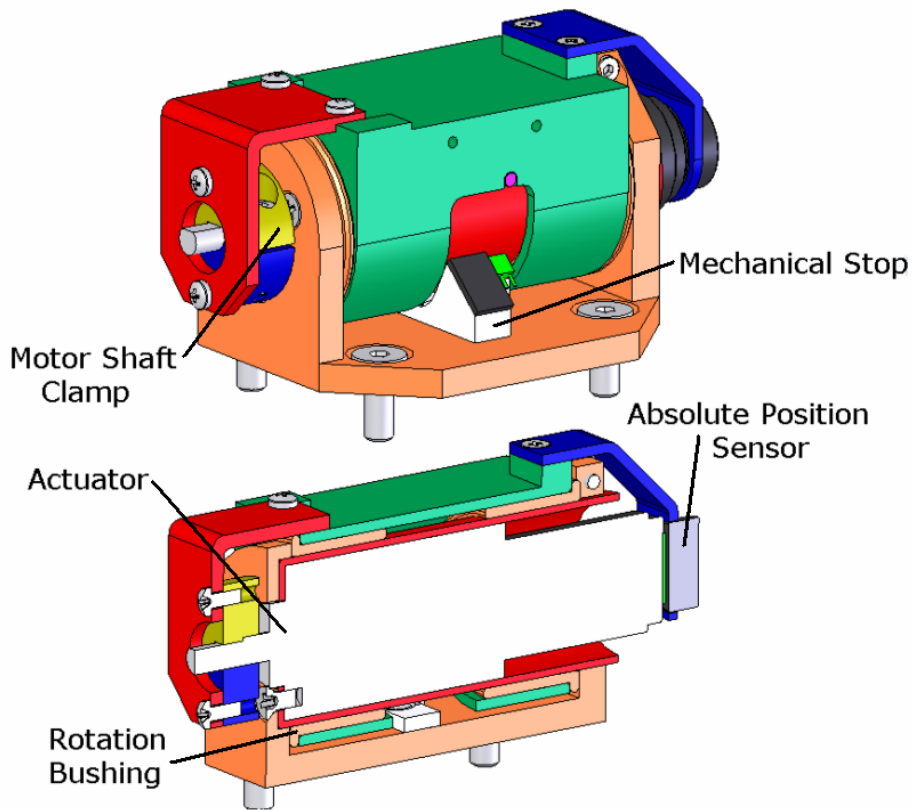


Figure 31: CAD Model of the Tilt Actuation Module of the Neck Mechanism

One major requirement of this system is the resilience to damage of the robot units since learning (cognition, understanding, and behavior) of the robot will potentially involve many “falls” and “accidents” experienced by any child learning to cope with the world. This may be particularly critical for the delicate head and neck mechanisms.

To overcome this problem, the pan joint in the serial neck mechanism uses an overload clutch system (Figure 32) since its actuator's gearbox is the weakest one and would not resist to an impact situation. The Overload Clutch System is essentially composed by a driven component, which is fixed to the driven part of the mechanism, a nut, a belleville spring and a clamp device, fixed to the motor shaft. When the belleville spring is compressed by the nut, the driven component is

smashed against the clamp device, producing enough friction to transmit the movement of the joint. In an overload situation, this friction will not be enough and the driven component will slide, protecting the motor gearbox from the impact.

The overload clutch system increases the robustness of the mechanism, giving it the possibility to fall on the floor and suffer different kind of impacts and efforts during its interaction with the external world.

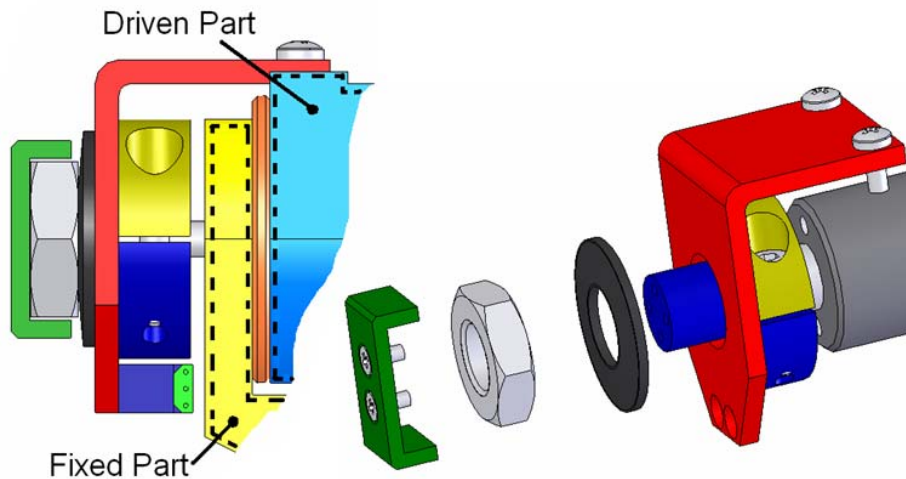


Figure 32: Clutch based overload protection system.

The belleville springs are shaped like a coned disk and especially useful where large forces are desired for small spring deflections.

Two of the critical parameters affecting the Belleville spring are the diameter ratio, R_d , and the height-to-thickness ratio h/t (Figure 33).

$$R_d = \frac{D_0}{D_i} \tag{15}$$

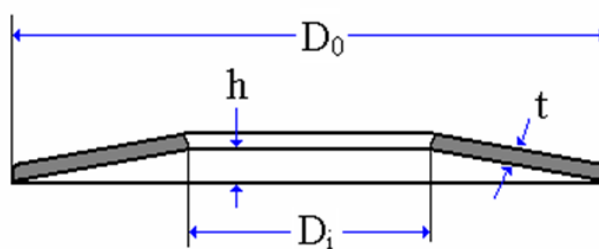


Figure 33: Typical Belleville Spring.

From Figure 34 the behaviour of a Belleville spring is highly nonlinear and varies considerably with the change in h/t. For low h/t values the spring acts almost linearly, whereas large h/t values lead to highly nonlinear behaviour. The force-deflection curves for Belleville springs are given by

$$P = \frac{4E\delta}{K_1 D_0^2 (1-\nu^2)} \left[(h-\delta) \left(h - \frac{\delta}{2} \right) t + t^3 \right] \quad (16)$$

where E is the elastic modulus, δ is the deflection from the unloaded state, D_0 is the coil outside diameter, ν is Poisson's ratio for the material, h is the spring height, and t is the spring thickness. The factor K_1 is given by

$$K_1 = \frac{6}{\pi \ln R_d} \left[\frac{(R_d - 1)^2}{R_d^2} \right] \quad (17)$$

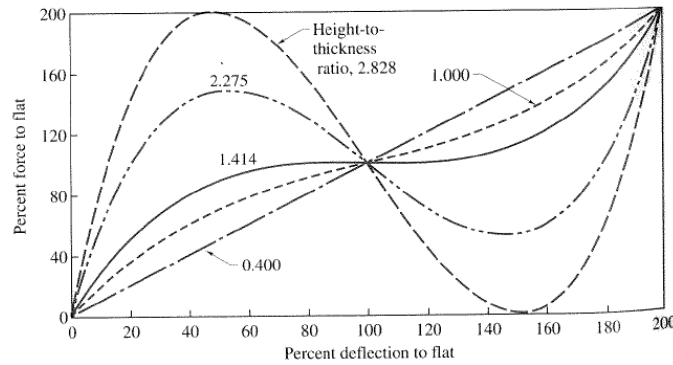


Figure 34: Force-deflection of Belleville Spring.

Considering T_M (Nm) to be the maximum allowable torque that the gearbox of the actuator can support, the desired P is

$$P = \frac{T_M}{\pi \mu r_i (r_0^2 - r_i^2)} \quad (18)$$

where μ is the friction coefficient of the spring's material.

Using equations (18), (17) and (16) the optimal deflection of the Belleville Spring, from the unloaded state, can be calculated (Table 5).

T_M (mNm)	600
μ	0.2
D_0 (mm)	18
D_1 (mm)	8.4
t (mm)	0.0010
h (mm)	0.0014
Rd	2.25
K1	0.73
P (mN)	4515
δ (mm)	0.0006

Table 5: Calculation of the ptimal deflection of the Belleville Spring for clutch system

As the thread pitch of the M8 nut, used in the clutch system, is 1.25 mm, it should be rotated 180° to guarantee the correct deflection, δ , of the Belleville Spring.

3.2. Eyes Mechanism

The eyes cyclotorsion was ignored because it is not useful for control, and similar image rotations are easily produced by software. The elevation/depression from both eyes is always the same in humans, in spite of the existence of independent muscles. Similarly, a single actuator is used for the robot eyes elevation (tilt). Eye vergence is ensured by independent motors. Figure 35 shows the final chosen kinematics, that allows all basic ocular movements.

The pan movement is driven by a belt system, with the motor behind the eye ball (Figure 36). The eyes (common) tilt movement is actuated by a belt system placed in the middle of the two eyes. Each belt system has a tension adjustment mechanism.

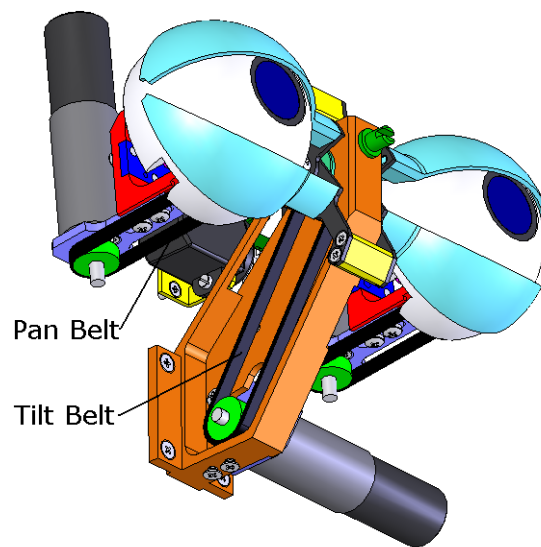
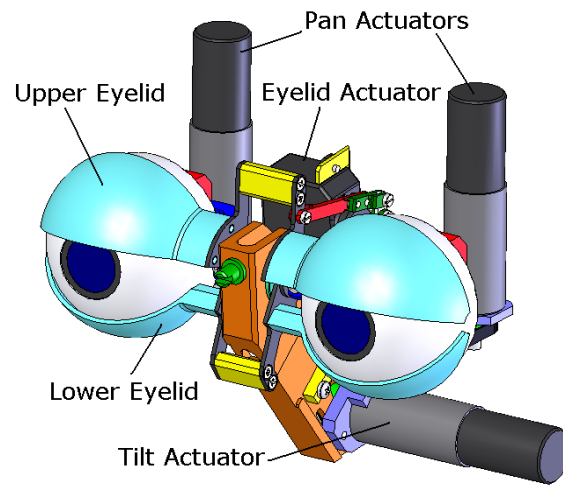


Figure 35: Eyes mechanism

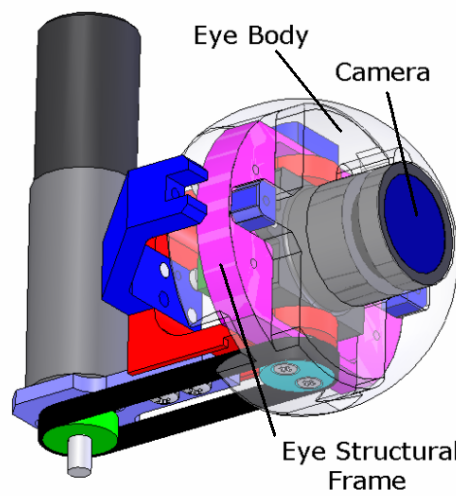


Figure 36: Single Eye Mechanism

3.3 Actuators Selection

The selection of actuator and reduction ratio is an important issue in the design of a humanoid robot. The reason is that the more powerful actuators are selected, the heavier the humanoid is constructed, and therefore, the more powerful actuators are required. To optimize the selection of actuators and reduction ratios, iterations of mechanical design are necessary.

Several analytic calculations and dynamic simulations were carried out on the neck and head motions including the six specified degrees of freedom, defined in Section 2.2. The results of calculations were obtained from simulating the robot head moving its 6 joints in the most critical movements, with the maximum acceleration and gravity forces.

These results gave us the guidelines to decide hardware specifications such as actuators, reduction ratios of gears and pulleys and other kind of mechanical components. By comparing data present on standard actuators catalog and that obtained from the calculations and simulations, we finally decided the hardware specifications on motors, gear boxes and encoders.

Since electrical motor control is relatively easy and has been widely studied, it was decided by the RoboCub Consortium to use it for the icub actuation. So, as the DC motors are fairly compact, we decided to use Faulhaber DC Micromotors, connected with Faulhaber and Gysin Planetary Gearheads and Faulhaber Magnetic Encoders (Figure 37).

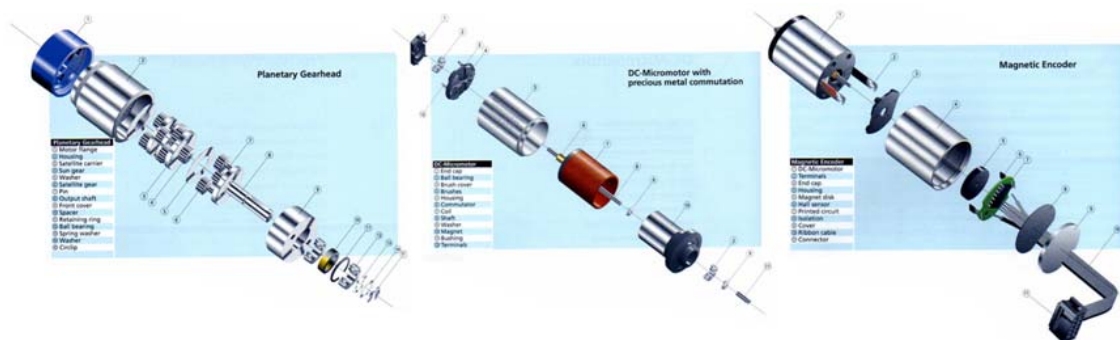


Figure 37: Faulhaber DC Micromotors, Gearheads and Magnetic Encoders

The joints of the Neck and Eyes Mechanisms can be represented by the following way:

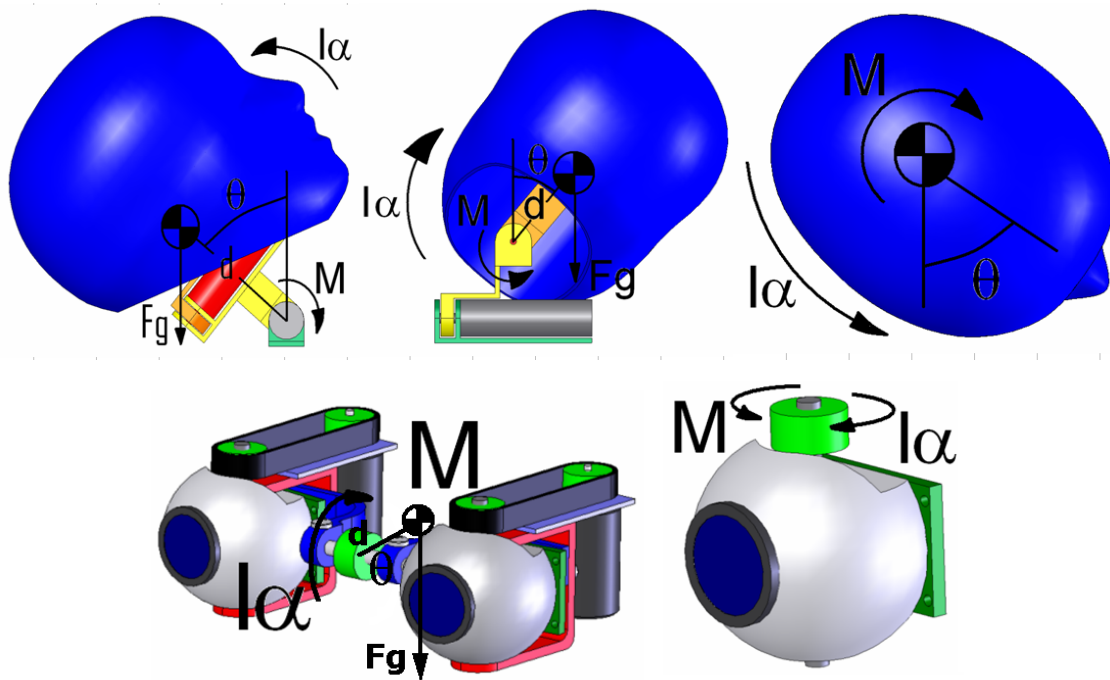


Figure 38: Joints representation

, where:

- **T** is the torque of the motor, that we want to calculate,
- α is the maximum acceleration for each joint, calculated in Section 2.2,
- θ is the maximum rotation of the joint from the vertical position. In the calculation the worst-case scenario of the value was changed to 90 degrees, since it should be very frequent, e.g. when the robot is crawling.
- **d** is the distance of the center of gravity of the rotating part to the axis of rotation of each joint. The exact value is given by *SolidWorks*,
- **Fg** is the weight of the rotating part of each joint, whose value is given by *SolidWorks*,
- **I** is the moment of inertia of the rotating part of each joint about the rotating axis. The exact value is given by *SolidWorks*,

So, for a general situation, we have:

$$T = Fg \cdot d + I \cdot \alpha \quad (19)$$

The two members of the right side part of the equation correspond, respectively, to the gravity and inertia part of the required torque. The calculations showed us that

the gravity part is much more relevant than the inertia one.

Computing the previous formula for the 5 different joints of the mechanisms, we got the values presented in Table 6.

Joint		d (m)	m (Kg)	Fg (N)	I (Kg.m ²)	θ (°)	a (rad/s ²)	T (mNm)
Neck	Pan	0.022	1.1	10.78	0.003	90	5.1	252.6
	Tilt	0.088	1.34	13.13	0.014	90	4.2	1214.6
	Swing	0.064	1.24	12.15	0.007	90	3.7	803.9
Eyes	Pan	0.007	0.036	0.35	6.50E-06	90	25.1	2.6
	Tilt	0.012	0.13	1.27	8.60E-05	90	22.3	17.2

Table 6: Torque calculation for mechanism joints

After getting these values of the required torques for the different joints, the actuators (motor + gearbox + encoder) were chosen from the catalog and are presented in Table 7.

Joint		Motor		Gearhead		Encoder
		Company	Ref.	Ref.	GR	Ref
Neck	Tilt	Faulhaber	1724024SR	Gysin GPL 22	343	IE2-512
	Swing	Faulhaber	2224024SR	Gysin GPL 22	245	IE2-512
	Pan	Faulhaber	1717024SR	Faulhaber 16/7	246	IE2-512
Eyes	Tilt	Faulhaber	1319024SR	Faulhaber 14/1	246	IE2-400
	Pan	Faulhaber	1319024SR	Faulhaber 14/1	66	IE2-400

Table 7: Actuator references for the 3 different joints of the neck mechanism

The final characteristics of the actuators are presented in Table 8:

Joint		Final Characteristics					
		Torque (Nm)	Vmax (°/s)	A.max (°/s ²)	T.avail (Nm)	Backlash (°)	Resolution (°)
Neck	Tilt	1.215	105	285	1.225	≤0,5	0.002
	Swing	0.804	147	1922	1.041	≤0,5	0.003
	Pan	0.250	122	1115	0.295	≤1	0.003
Eyes	Tilt	0.017	189	180000	0.186	≤1	0.006
	Pan	0.003	455	658000	0.077	≤1	0.014

Table 8: Actuator Final Characteristics for the 3 different joints of the neck mechanism

Comparing these final values with the specified ones, presented in section 2.2, it can be seen that the maximum velocities and accelerations not only satisfy the specified ones but exceed them, approaching the maximum values of an adult human.

3.4. Eyelid Mechanism

The concept of this eyelid mechanism was inspired in a classic mechanical linkage mechanism: the Four Bar Mechanism, Figure 39. It consists of 4 rigid bodies (called bars or links), each attached to another two, by single joints or pivots to form a closed loop. Planar four-bar linkages perform a wide variety of motions with a few simple parts. They are also popular due to ease of calculations, compared to more complex mechanisms.

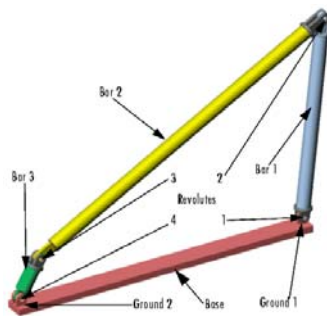


Figure 39: Typical configuration of a Four Bar Mechanism

As can be shown in Figure 40, the Eyelid Mechanism is composed by two Four Bar Mechanisms working in parallel, having just 1 DOF - an upper one, for the upper eyelid system, and another for the lower eyelid system. The length of the different links was optimized to transform the servomotor input (which is the same for both eyelids) in a different output, altering the motion, velocity and acceleration of the upper and the lower eyelids.

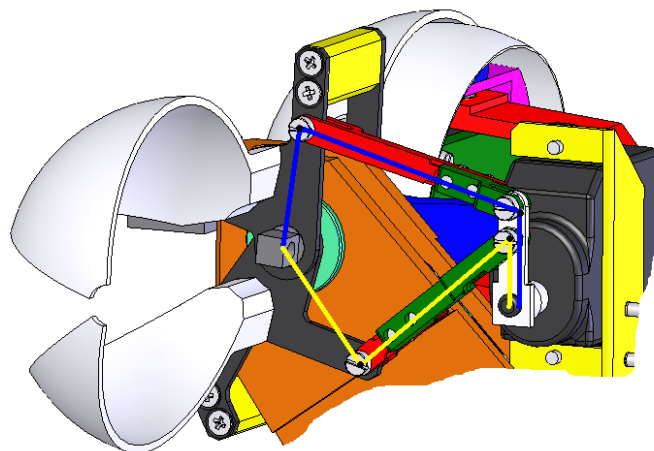


Figure 40: The Eyelid Mechanism composed by the two parallel Four Bar Mechanisms (the upper eyelid system in blue and the lower eyelid system in yellow)

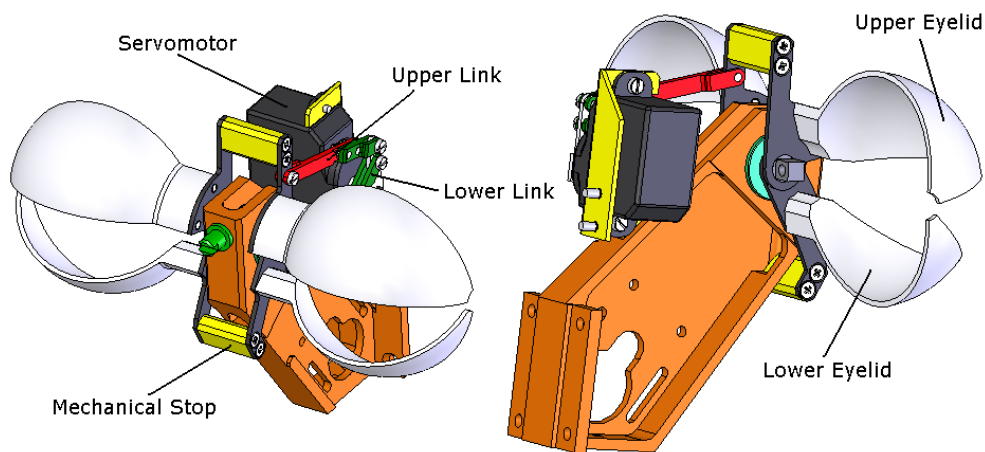


Figure 41: Different views of the Eyelid Mechanism

To guarantee the spherical concentricity of the eyes and the eyelids, and to increase the compactness of the mechanism, the eyelids system shares the shaft of rotation with the eyes system.

The left and right eyelids are fixed by the two yellow aluminium components shown in Figure 41.

In order to allow little improvements of the eyelids position, the upper and the lower link's length can be changed by an adjustment system, Figure 42.

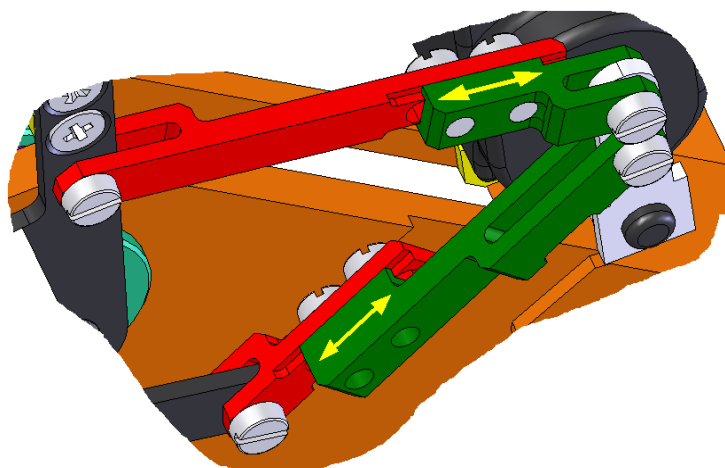


Figure 42: Link Adjustment System

Apart from the eyelids, all mechanical components of the system are aluminium machined parts.

Due to its complex geometry, the eyelid components (Figure 43) are produced by an SLS process, the same used for the production of the Head Cover. They are glued to the mechanism by cyanoacrylate glue and its correct position is guaranteed by two positioning pins, which are part of the eyelid components.

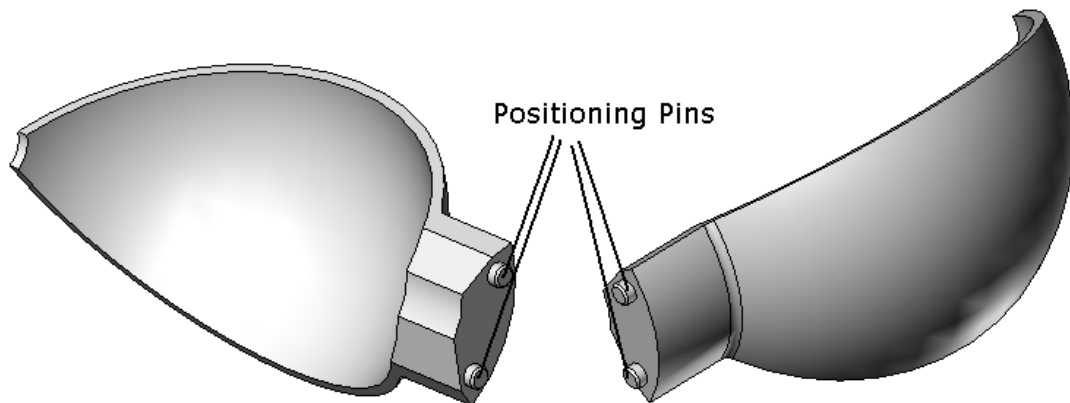


Figure 43: Eyelid geometry

In the actuation of this mechanism, we are using a Futaba S3111 (Figure 44) servomotor; which is a cheap, small, light and relatively high torque solution.

Specifications:

Length: 21.8mm

Width: 11mm

Height: 19.8mm

Weight: 6.6g

Speed: 12 sec/60°

Torque: 60 mNm



Figure 44: Futaba servomotor (<http://www.futabarc.com/servos/servos.html>)

In the configuration of the mechanism, the servo has a range of movement of 75°, from the closed eyelid position to a maximum opened eyelid position.

3.5. Material Selection

The data given in Figure 45 allow a preliminary assessment to be made of several materials of interest, showing the strength of several materials plotted against density.

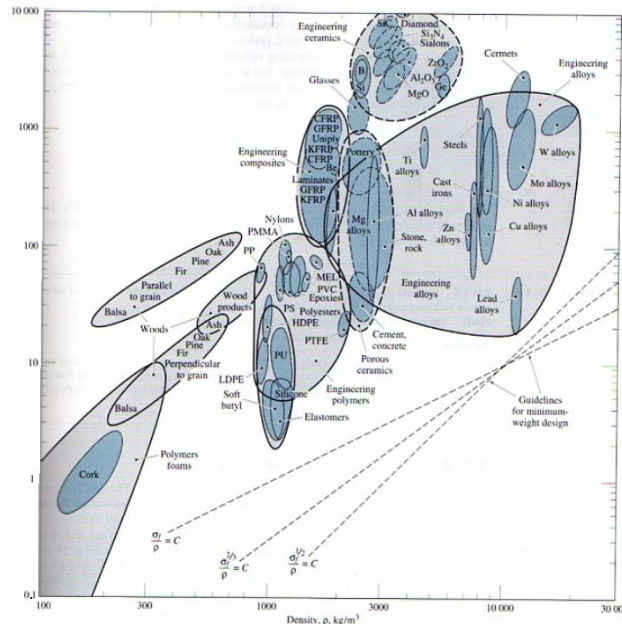


Figure 45: Strength of several materials plotted against Density

The high density of steel- nearly 3 times that of Aluminium- would seem to make it a poor prospect for use in robotic systems, and yet it has been used quite extensively. That is especially because of its high strength and production facilities. On this specific design, excluding the screws, washers, nuts, pins and shafts, steel (303SS) was used in very thin parts and in small threaded components.

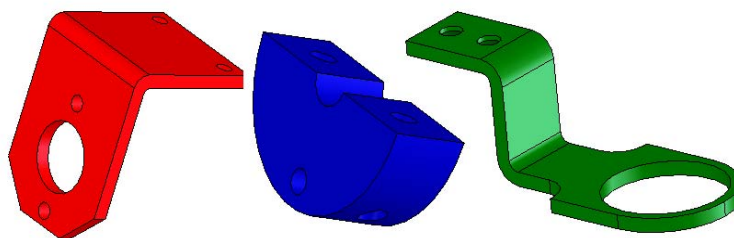


Figure 46: Some steel components of the head mechanism

Aluminium alloys are still the major materials for robotic systems construction, and seem likely to remain so for the foreseeable future, although the proportion of total take-off weight which they represent will no doubt progressively decrease due mainly to competition from composites. As shown in Figure 45, in terms of

strength/density ratio, aluminium alloys can be superior to steel.

Another advantage from steel is the fact that aluminium alloys are corrosion resistant.

So having in mind all this information, the majority of the components of the system were produced in aluminium (Al 7075-T6), especially the bigger and more complex structural parts.

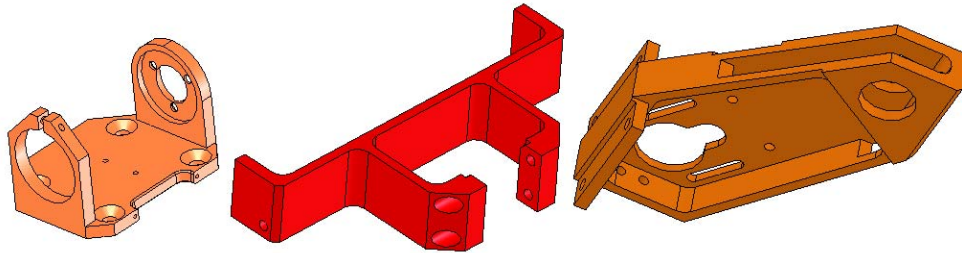


Figure 47: Some aluminum components of the head mechanism

Plastics can offer improved specific properties compared with steel, thereby saving weight (nearly 6 times less). They can resist corrosion, can have a high quality surface finish and can be much more easily machined. However, it is not recommended to thread them and they can not guarantee a high level of geometric tolerances. So, plastic components were only used in big non structural, and non threaded, parts, like the eye balls of the robot.

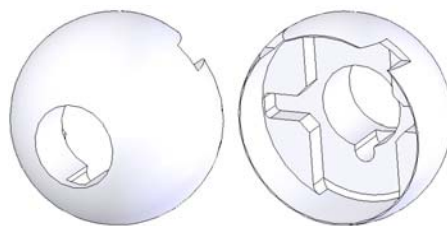


Figure 48: A plastic component of the head mechanism

3.6. Assembly

As an open physical platform for embodied research, that can be used by the research community from different types of science fields (like physiology, cognitive robotics and perceptual science), the iCub mechatronics system cannot be very complex. So, in order to guarantee easy assembly and maintenance procedures, the mechanical system architecture is also completely modular, in such a way that

we can remove and replace a certain module, without having to disassemble the entire structure. Figures 49 and 50 show the different modules of the head, and the integration with electronics.

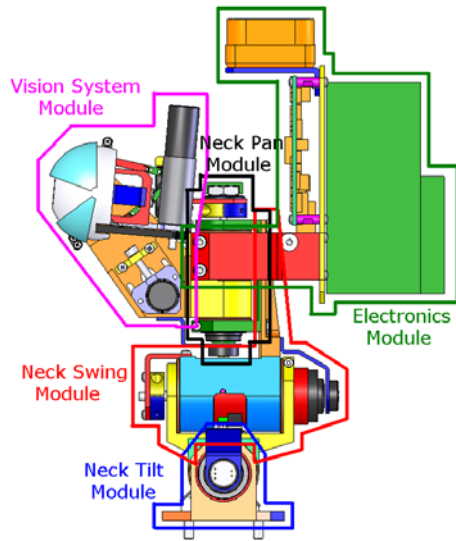


Figure 49: Modular Architecture of the System

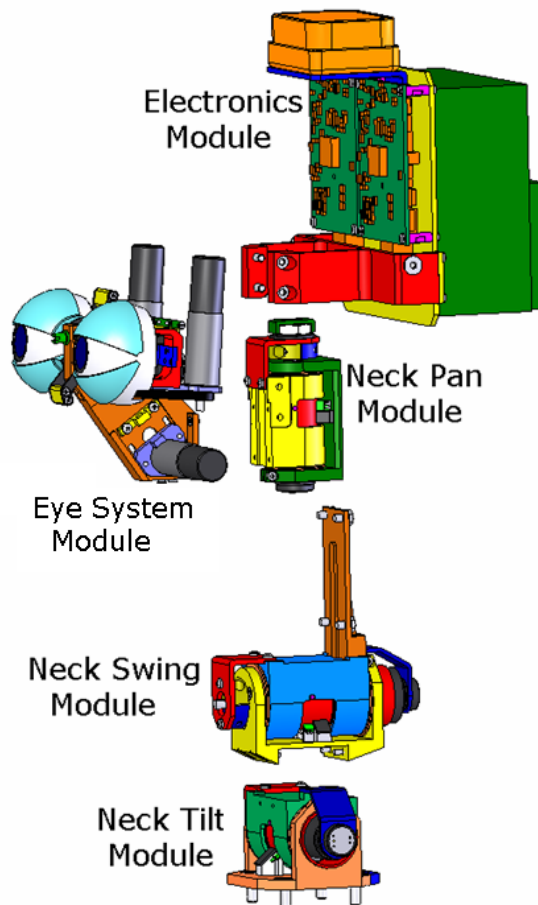


Figure 50: Exploded View of the head mechanism

3.7. Sensors and Electronics

To allow the robot to interact with other people and to have all desired behavior several sensors were applied.

For vision, the main sensory modality, two DragonFly cameras [www.ptgrey.com] with VGA resolution and 30 fps speed. These cameras are very easy to integrate because the CCD sensor is mounted on a remote head, connected to the electronics with a flexible cable. In this way, the sensor head is mounted in the ocular globe, while the electronics are fixed to a non-moving part of the eye-system.

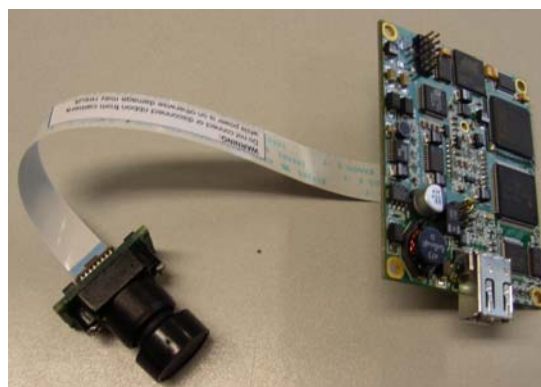


Figure 51: DragonFly Camera (sensor head and electronics connected by a flexible cable)

The inertial sensor is very important to have the vestibuloocular reflex and to detect the overall posture of the body. We have selected the from MTi sensor, from Xsens Technologies B.V. It is a miniature, gyro-enhanced Attitude and Heading Reference System. Its internal low-power signal processor provides drift-free 3D orientation as well as calibrated 3D acceleration, 3D rate of turn (rate gyro) and 3D earth-magnetic field data.

The MTi uses 3 rate gyros to track rapidly changing orientations in 3D and it measures the directions of gravity and magnetic north to provide a stable reference. The systems real-time algorithm fuses the sensor information to calculate accurate 3D orientation, with a highly dynamic response and stable over time.



Figure 52: MTi sensor

All motor control boards will be specially designed to fit in the size constraints of the robot. They are all integrated in the head and connect to the remote computer with CANbus.

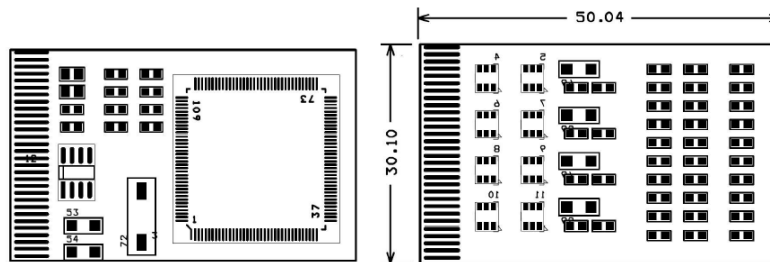


Figure 53: Motor control boards

To measure the head position (kinesthetic information), the motors have magnetic encoders, for calibration purposes absolute position sensors were applied to each neck joint. GMW Associates (www.gmw.com) has available a sensor, the GMW360ASM, capable of 360° angular sensing with linear output. It is a cylindrical package with 12.7mm diameter and 5 mm thick. It is constituted by two hall sensors in quadrature and a microprocessor that computes the direction of the magnetic field based on the quadrature measurements. The GMW360ASM provides an Analog and PWM output signal which is proportional to the mechanical angle of a magnet with a resolution of 0.75 degrees. In addition to the absolute angle position outputs, the GMW360ASM detects when the field strength of the magnet is too low and provides a discrete "Magnet Out of Range" signal. The electrical "Zero Angle" position can be set to correlate to any mechanical position within 360 degrees. This is accomplished by momentarily connecting the Analog Output pin to the +5 Volt supply and applying power.

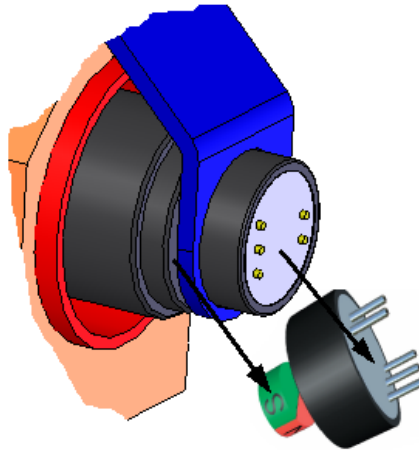


Figure 54: Absolute position sensor

The electrical output of the module for the zero angle position can be set to match any mechanical position of the magnet within the 360 degree rotation. This feature eliminates the need to mechanically align the position of the sensor output to the mechanical position of the rotating target. The zero angle output is 2.5V for the Analog Output and 50% Duty Cycle for the PWM output. The Zero Angle set function is initiated by providing a momentary connection between the Analog Output pin and the 5V supply prior to applying power to the module. Once power is on for more than 100 ms, the momentary connection is removed and a 100 ms "Zero Angle" calculation is initiated. At the end of the 100 ms time, the GMW360ASM is operational and the Analog Output will be set to 2.5V and the PWM output will be set to 50% Duty Cycle. The Zero Angle set point is permanently stored into flash memory and remains there until a new Zero Angle command is initiated. The maximum number of changes to this set point is 50000.

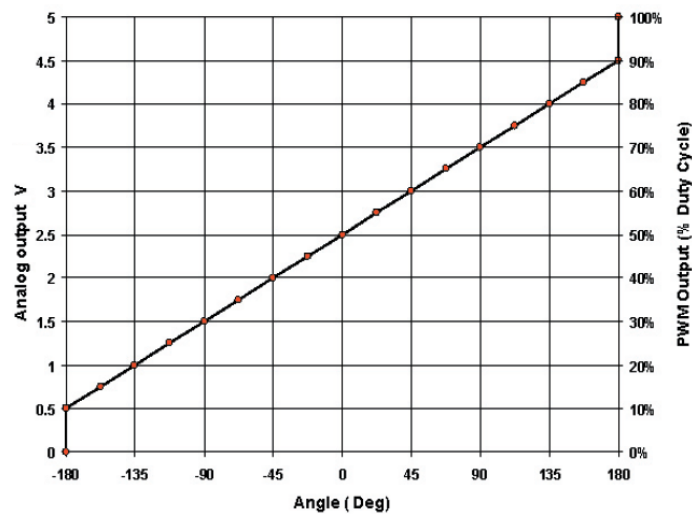


Figure 55: GMW360ASM Output characteristics

3.6 External Cover

Since this robot is designed to be engaged in social interaction, one of the main concerns in the design is the understanding of which facial features dimensions contribute more to the communication with humans. This research is important for the fields of human-computer interaction and the impact of design on this field has to be well understood.

There are several studies [DiSalvo et al., 1993], [Takeuchi et al., 1995] that show that the presence of certain features, the general dimensions of the head, and the number of facial features greatly influence the perception of humanness in robot heads. Some robots are much more successful in the portrayal of humanness than others. This success is due, at least in part, to the design of the robot's head.

Masiro Mori developed a theory of The Uncanny Valley (Figure 56), which states that as a robot increases in humanness there is a point where the robot is not 100% similar to humans but the balance between humanness and machine-like is uncomfortable, and so, there is a reasonable degree of familiarity that should be achieved and maintained in humanoid robots [Reichard, 1978].

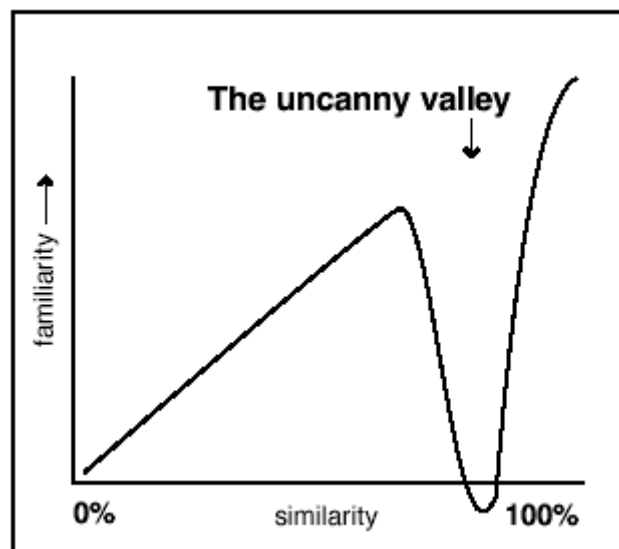


Figure 56: Mori's The Uncanny Valley [Reichard, 1978].

The external cover must also ensure the protection of head mechanisms, absorbing external efforts, suffered by the robot during operation. Figure 57 shows the first prototype of the iCub face, where a "toy-like" concept was selected for the design.

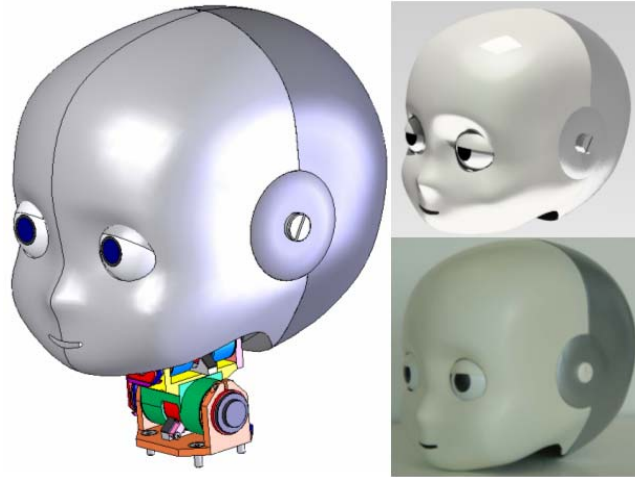


Figure 57: Preliminary Design of the iCub external cover (made by AlmaDesign).

In order to accurately estimate the location of a sound source in both the horizontal and vertical plane, two human-like ears of simple spiral-shaped, with a microphone on the center, were designed and added to the final version of the iCub external cover (Figure 58).

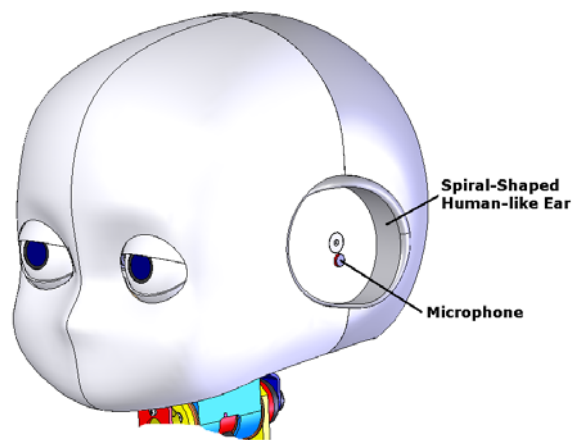


Figure 58: Final Design of the iCub external cover

4. Performance

Several tests were made to evaluate the functional use of the designed head. Every joint was tested, in the worst case scenario, to verify that velocity and acceleration specification were met. Several other demos/tests were created to verify the coordination between the sensors and actuators in the system.

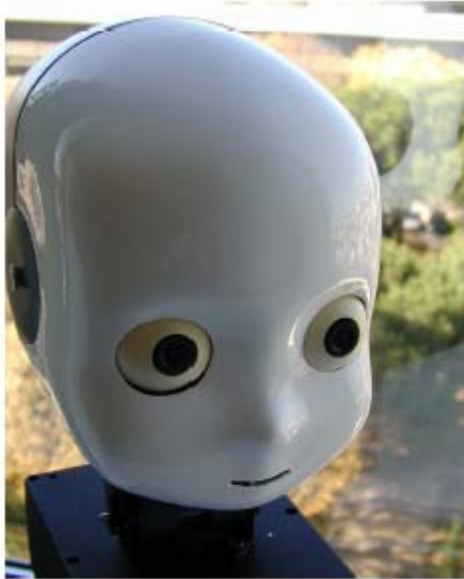


Figure 59: Final prototype of the iCub head with face

1) Mechanical performances - In order to simulate the hardest working situations of the mechanism, its base was fixed in a vertical position, as shown on Figure 60.

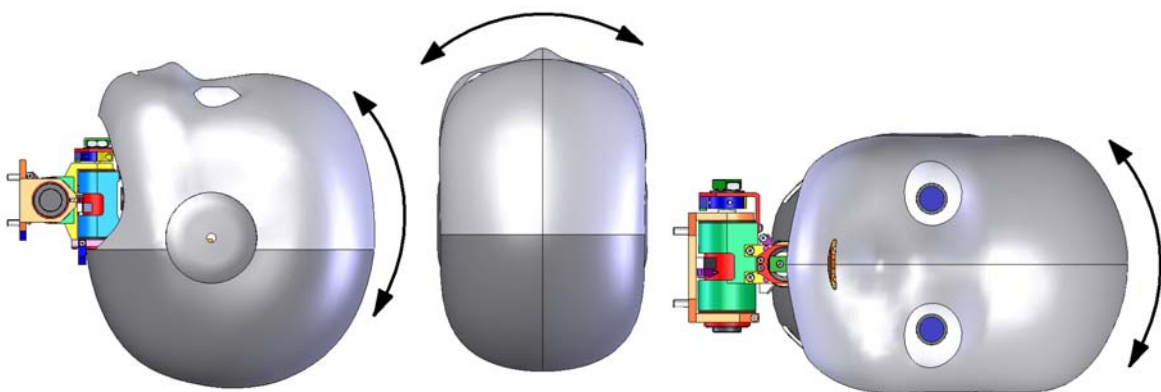


Figure 60: Movements made during the mechanical tests

The weight of the head components was measured before the realization of the

mechanical tests. The values are shown on Table 9.

Component's Weight (g)	
Cover	257
Mechanism	1104
Extra Payload (Full)	340
Total	1701

Table 9: Weight measurement

The test of each dof was made using the following procedure:

Static Test

1. The head was fixed on its homing position, with zero velocity, full load (payload=340g), for a short period of time (t= 5s);

Dynamic Test

2. The head was moved, with its maximum velocity, along its total range of movement, with full load, for a short period of time;

Endurance Test

3. The head was moved, with its maximum velocity, along its total range of movement, with full load, for 30 min, verifying the temperature of the actuator;

Joint	Payload (g)	Vel (rad/s)	Test Period (s)	Real Range of Movement (°)	Obs
Tilt	340	0	5	+40; -50	✓
		1.3	5		✓
		1.3	1800		✓
Swing	340	0	5	+40; -40	✓
		1.2	5		✓
		0.1	5		✓
Pan	340	0	5	+55; -55	✓
		1.6	5		✓
		1.6	1800		✓

Table 10: Different tests Summary

After these experimental tests (Table 10), we could conclude that, the neck actuators were able to move the head, during 30 min, with full load.

2) Object tracking- An object moving in front of the system is considered to be successfully tracked if it is near the center of both images. Since this is a 3 dof task and the robot has 6 dof, some extra criteria should be used to control all dof. The eye's 3 dof are directly controlled with a visual servoing mechanism, having the image positions of the object as feedback. The neck is then controlled in order to maintain the eyes as far as possible for their joint limits. This choice is motivated by biological behavior. The rationale for having the eyes in a comfortable position is that they will be readily available to track the object in any direction even if it moves very fast (Figure 61).



Figure 61: Light tracking test

3) Balancing - The inertial sensor provides a reliable measure of the orientation of the head and also the angular velocities. This information can be used to keep the head always in a upright position. The inclination information controls directly the first 2 dof of the neck. The angular velocity is used to create an artificial vestibular reflex that in presence of a fast motion keeps the eyes looking in the same direction (Figure 62).



Figure 62: Balancing test

4) Sound localization - Using information about the time difference, sound energy level and spectral power at some special frequencies, it is possible to localize sound sources with the iCub head. This algorithm is very reliable for the horizontal plane and can be used either with a closed or an open loop controller (Figure 63).

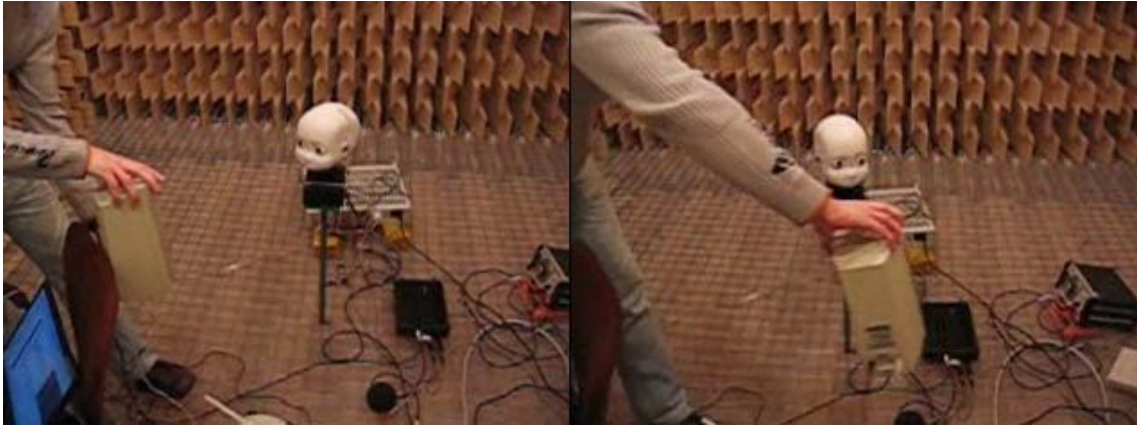


Figure 63: Sound localization test

5. Conclusions/ Future Work

We presented the design for a robot head of a small size humanoid robot. This humanoid robot - the iCub - is meant to be used as a research tool for human cognition and publicly distributed worldwide. The iCub neck has 3 dof and the eyes 3 dof, the more complex mechanism for similarly sized robots, where the eyes are usually fixed.

The specifications were derived from human anatomical and behavioral data. As some of these data are not available (and even less data can be found for children), extra assumptions had to be made. We referred to typical tasks the robot should do and the ratio between neck and eyes velocities/acceleration in humans. The final kinematic has three dof for the neck. For the eyes, three degrees of freedom (independent vergence, common tilt) were considered. Other movements like cyclotorsion can be dealt with at the camera level.

A first solution for the neck was a spring mechanism mimicking the human anatomy. It has good kinematic capabilities but low repeatability and precision, due to the spring.

A very small 3 dof parallel actuator was proposed as our second design. It is very compact and delivers high torque. Due to extremely reduced size, a ball screw linear actuator was designed. It meets all the specifications, except the desired range of motion. Although this could be a very attractive solution if we could afford using a 20% bigger neck, self interference of the mechanical parts precluded its use at the current stage.

The design that met all the specifications was a serial mechanism. It has a clutch system to overdrive protection. All motors are similar and the assembly is modular.

As can be seen in Table 11, the dynamic performance of the mechanism not only satisfy the specified values, presented in section 2.2, but exceed them, approaching the maximum values of an adult human.

Joint		Torque (Nm)			Vmax (°/s)			Amax (°/s ²)		
		Specified	Final	Increase (%)	Specified	Final	Increase (%)	Specified	Final	Increase (%)
Neck	Tilt	1.215	1.225	1	73.6	105	43	241	285	18
	Swing	0.804	1.041	29	65.5	147	124	214	1922	797
	Pan	0.250	0.295	18	90.0	122	36	295	1115	279
Eyes	Tilt	0.017	0.186	994	160.0	189	18	1280	180000	13963
	Pan	0.003	0.077	2467	180.0	455	153	1440	658000	45694

Table 11: Specified vs. Final dynamic performance of the mechanism

The lightweight eye system has three dofs, consisting of independent eye pan and a common tilt. The head is equipped with additional sensors, like an inertial sensor for the vestibular system, kinesthetic information from encoders, absolute position sensors in the neck and embedded controllers.

A first prototype of the iCub face was designed and built. The head has been mounted and tracking experiments were done to assess the performance of the mechanism that is quite encouraging.

As future work, some improvements can be done.

An important upgrade of this robotic head design could be the use of Harmonic Drive gear boxes (Figure 64) instead of planetary gear heads, since they have operating principles and construction processes that maximize output torque and minimize size and weight, offering advantages such as high reduction ratios in a single stage, zero backlash, and high precision that cannot be equaled by planetary gear trains.

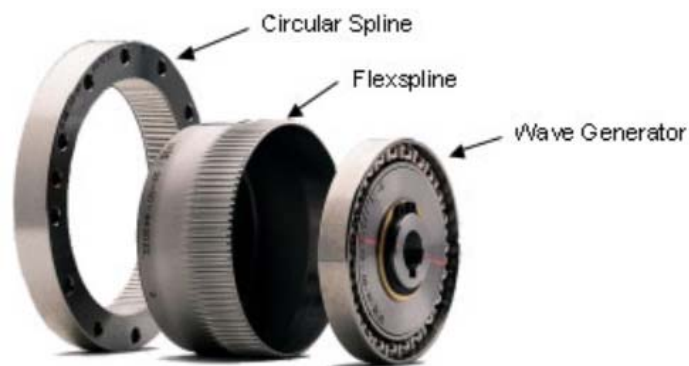


Figure 64: Harmonic Drive components

A re-formulation of the actuation modules could be conducted to a more efficient cable routing along the serial mechanism of the neck. This could have been achieved if the actuation modules had had enough space inside allowing the cable to flow near the center of rotation of the different joints.

Nine units of this head mechanism have already been reproduced in different countries and the iCub final mechanical design will be freely available to researchers worldwide, and released under General Public License (GPL) - www.robotcub.org.

6. References

- [Alici et al., 2004] Gursel Alici and Bijan Shirinzadeh. Topology optimisation and singularity analysis of a 3-SPS parallel manipulator with a passive constraining spherical joint. *Mechanism and Machine Theory*, 39:215–235, 2004.
- [Beira et al, 2005] Ricardo Beira, Manuel Lopes, Miguel Praça, José Santos-Victor, Alexandre Bernardino, Giorgio Metta, Francesco Becchi, Roque Saltarén, Design of the Robot-Cub (iCub) Head, ICRA - IEEE International Conference on Robotics and Automation, Orlando, USA, 2006
- [Geppert, 2001] L. Geppert. Qrio, the robot that could. *IEEE Spectrum*, 41(5):34–37, May 2004.
- [DiSalvo et al., 1993] Carl F. DiSalvo, Francine Gemperle, Jodi Forlizzi, Sara Kiesler, All Robots Are Not Created Equal: The Design and Perception of Humanoid Robot Heads. In *Proceedings of INTERCHI '93*, (Amsterdam, the Netherlands, 1993), ACM Press: New York, 187-193.
- [Gregorio, 2003] Raffaele Di Gregorio. Kinematics of the 3-UPU wrist. *Mechanism and Machine Theory*, 28:253–263, 2003.
- [Gregorio, 2004] Raffaele Di Gregorio. Statics and singularity loci of the 3-UPU wrist. *IEEE Transactions on Robotics*, 20(4), 2004.
- [Hirose et al., 2001] M. Hirose, Y. Haikawa, T. Takenaka, and K. Hirai. Development of humanoid robot ASIMO. In *Workshop on Exploration towards Humanoid Robot Applications at IROS*, Hawaii, USA, 2001.
- [Laananen, 1999] D. Laananen. Computer simulation of an aircraft seat and occupant in a crash environment. Program som-la/som-ta user manual, US Department of Transportation, Federal Aviation Administration, 1999.
- [Lopes et al., 2004] Manuel Lopes, Ricardo Beira, Miguel Praça, José Santos-Victor, An anthropomorphic robot torso for imitation: design and experiments, IROS - IEEE/RSJ International Conference on Intelligent Robots and Systems, Sendai, Japan, 2004

- [Merlet, 2001] Merlet, J., Parallel Robots. Kluwer Academic Publishers, 2001
- [Netter, 1998] Frank Netter. Atlas of Human Anatomy. third edition, Learning Systems
- [Panero et al., 1979] Julius Panero and Martin Zelnik. Human Dimension and Interior Space: A Source Book of Design Reference Standards,. Watson-Guption Pubs, 1979.
- [Reichard, 1978] Reichard, J. Robots: Fact, Fiction, and Prediction. Penguin Books, 1978.
- [Sandini et al., 2004] Giulio Sandini, Giorgio Metta, and David Vernon. Robotcub: An open framework for research in embodied cognition. International Journal of Humanoid Robotics, 8(2), November 2004.
- [Silva, 2003] Miguel Silva. Human Motion Analysis Using Multibody Dynamics and Optimization Tools. PhD thesis, Instituto Superior Técnico, Lisboa, Portugal, 2003.
- [Takeuchi et al., 1995] Takeuchi, A. and Naito, T., Situated Facial displays: Towards Social interaction. In Proceedings of Human Factors in Computing Systems '95, (1995), ACM Press: New York, 450-455.
- [Tilley, 2001] Alvin R. Tilley. The Measure of Man and Woman: Human Factors in Design. Henry Dreyfuss, 2001.
- [Yamasaki et al., 2000] F. Yamasaki, T. Miyashita, T. Matsui, and H. Kitano. PINO the humanoid: A basic architecture. In Proc. of The Fourth International Workshop on RoboCup, Melbourne, Australia, August 2000.
- [Zangemeister et al., 1981] Zangemeister and Stark. Active head rotations and eye-head coordination. Ann N Y Acad Sci, 374:540-59, 1981.
- [Zatsiorsky, 1997] Vladimir Zatsiorsky. Kinematics of Human Motion. Human Kinetics Europe Ltd, 1997.